# A Benders Decomposition Approach for the Two-Echelon Stochastic Multi-period Capacitated Location-Routing Problem

Imen Ben Mohamed, Walid Klibi, Ruslan Sadykov, Halil Şen, François Vanderbeck

# A Benders Decomposition Approach for the Two-Echelon Stochastic Multi-period Capacitated Location-Routing Problem

Imen Ben Mohamed[1,2,3], Walid Klibi[1], Ruslan Sadykov[3,2], Halil Şen[4] and François Vanderbeck[5]

[1] The Centre of Excellence in Supply Chain (CESIT), Kedge Business School, France
[2] Mathematics Institute of Bordeaux (IMB),University of Bordeaux, France
[3] RealOpt, Inria-Bordeaux-Sud-Ouest, France
[4] Mapotempo, Bordeaux, France
[5] Atoptima, Bordeaux, France

July 9, 2019

**Abstract**

In the first echelon of the two-echelon stochastic multi-period capacitated location-routing problem (2E-SM-CLRP), one has to decide the number and location of warehouse platforms as well as the intermediate distribution platforms for each period; while fixing the capacity of the links between them. The system must be dimensioned to enable an efficient distribution of goods to customers under a stochastic and time-varying demand. In the second echelon of the 2E-SM-CLRP, the goal is to construct vehicle routes that visit customers from operating distribution platforms. The objective is to minimize the total expected cost. We model this hierarchical decision problem as a two-stage stochastic program with integer recourse. The first-stage includes location and capacity decisions to be fixed at each period over the planning horizon, while routing decisions of the second echelon are determined in the recourse problem. We propose a Benders decomposition approach to solve this model. In the proposed approach, the location and capacity decisions are taken by solving the Benders master problem. After these first-stage decisions are fixed, the resulting subproblem is a capacitated vehicle-routing problem with capacitated multi-depot (CVRP-CMD) that is solved by a branch-cut-and-price algorithm. Computational experiments show that instances of realistic size can be solved optimally within reasonable time, and that relevant managerial insights are derived on the behavior of the design decisions under the stochastic multi-period characterization of the planning horizon.

## 1. Introduction

Distribution problems have drawn much attention over the last decades as their applications are of great interest for public and private sectors since companies are always looking for ways to improve the efficiency of their distribution networks in terms of location of their facilities and the transportation schemes they use. Vehicle-routing problems (VRPs) are among the most extensively studied class of distribution problems in the operational research literature where the aim is to compute a set of minimum-cost routes to meet customer demands using a fleet of vehicles [21, 61]. Facility location problems (FLPs) have also been the subject of intensive research efforts. In the FLPs, locations of a set of warehouses need to selected from a finite set of potential sites and customers are served by direct routes from selected warehouses at the minimum cost possible [26, 22]. However, it is now commonly believed that the integration of the two decision levels into a location-routing problem (LRP), often leads to better network design solutions as introduced in [53] and recently discussed in [59, 32]. In LRPs, the aim is to find an optimal number of warehouses and their locations, while building routes around them to serve the customers. We refer the interested reader to [39] for an extensive literature review which includes descriptions of different location-routing applications and a classification scheme. However, as Drexl and Schneider [23] point out, most of LRP models studied so far consider a one-echelon distribution setting.

The growth of e-commerce in recent years and the emergence of omnichannel sales approaches have drastically changed the distribution landscape. They have significantly increased the delivery service level expectation and they favor a high proximity to customers' ship-to locations – e.g., home, stores, relay points [24]. Such challenges are especially experienced in urban areas due to the increase in city populations, which in effect leads to rising levels of congestion and more regulations to limit pollutant emissions. Therefore, practitioners, accepting the limits of

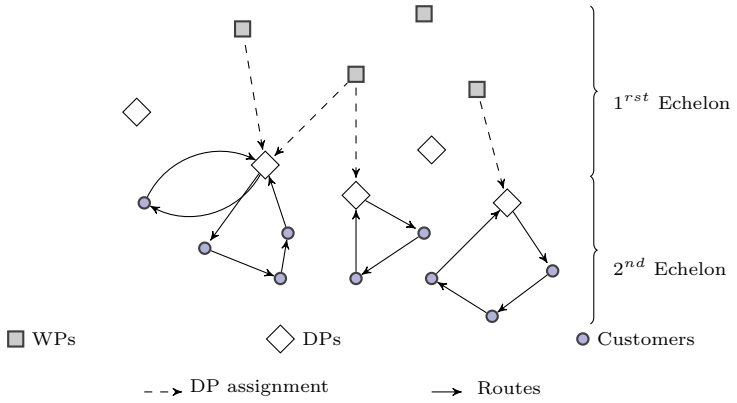


Figure 1: A potential two-echelon capacitated location-routing problem (2E-CLRP)

the one-echelon distribution networks, have nowadays turned their attention to two-echelon distribution structures to meet today's challenges. For instance, most of the retailers used to operate a single centralized warehouse per region/market that is optimized for risk pooling, sourcing and delivery efficiency. However, such warehouses are not necessarily optimized to provide next-day/same-day deliveries, or to efficiently operate fulfillment and shipment services for online orders. To deal with this problem, several retailers such as Walmart, JD.com or Amazon have reconfigured their distribution networks by adding an advanced echelon of distribution/fulfillment platforms, mostly in urban areas. According to Weinswig [66], Walmart plans to convert 12 Sam's Club stores into e-commerce fulfillment centers to support the rapid e-commerce growth. Two-echelon structure is nowadays promoted in several City logistics applications as well [19, 40]. This is done by creating peripheral distribution/consolidation centers, where freights coming from warehouses on large trucks are loaded into smaller and environmentally friendly vehicles, more suitable for city center distribution. Parcel delivery also represents a relevant application for the two-echelon capacitated location-routing [25]. Parcels travel from primary platforms to secondary distribution platforms, and they are then sorted and loaded onto smaller trucks that ship parcels to relay points, and to customers' homes. This is studied in [67], considering a route length approximation formulas instead of explicit routing decisions under a static-deterministic setting.

In this work, a two-echelon distribution problem is studied with the aim to design a network structure that offers more flexibility to the future business needs of a given company. More specifically, this strategic problem aims to decide the number and location of warehousing/storage platforms (WPs) and distribution/fulfillment platforms (DPs), and on the capacity allocated from first echelon to second echelon platforms. It also takes into account the transportation decisions between platforms. As consolidation is generally more pronounced at the primary echelon, we consider direct assignment with full truckloads transportation option departing from WPs to DPs. Then, since DPs are generally devoted to more fragmented services, the transportation activity from the second echelon is shaped by multi-drop routes. This problem description gives rise to the two-echelon capacitated location-routing problem (2E-CLRP). Figure 1 illustrates a typical 2E-CLRP partitioned into two capacitated distribution echelons: each echelon involves a specific location-assignment-transportation schema that must cope with the future demand.

Contrary to the VRP and the LRP, the literature on the 2E-CLRPs is very scarce. It is formally introduced by Sterle [60]. Later, it is studied by Contardo et al. [17] where the authors introduce a branch-and-cut algorithm based on a new two-index vehicle-flow formulation, strengthened by several families of valid inequalities. They also develop an Adaptive Large Neighborhood Search (ALNS) algorithm that outperforms the other heuristics proposed for the 2E-CLRP. Nguyen et al. [40, 41] examine a particular case of the 2E-CLRP with a single warehouse in the first echelon with a known position and proposed two heuristics to solve it. A literature survey on the two-echelon distribution problems can be found in [50], [23] and [20].

These models only consider the static and deterministic versions of the 2E-CLRP. However, given the strategic nature of the decision, it must be designed to last for several years, fulfilling future distribution requirements. To this end, the horizon must be partitioned into a set of periods shaping the uncertainty and time variability of demand and cost. The location and capacity decisions should be planned as a set of sequential decisions to be implemented at different design periods of the horizon (a year, for example) and promoting the structural adaptability of the network. This is more critical nowadays as distribution practices have got more complex over the years, and have higher uncertainty in terms of demand level, location, and cost evolution. Accordingly, the traditional deterministic-static representation of the planning horizon is due to be replaced by a more realistic stochastic and

multi-period characterization of the planning horizon. Hereafter, we refer to the stochastic multi-period version of the problem by the 2E-SM-CLRP.

Klibi et al. [31] examine a stochastic variant of the one-echelon LRP, but therein only the transportation level is decided under a multi-period setting, whereas in our study the multi-period feature involves the design decisions – i.e., location and capacity decisions). Ben Mohamed et al. [9] investigate a stochastic multi-period version of the two-echelon location-allocation problem, where routes are substituted by multi-period inter-facility flow decisions. To the best of our knowledge, stochastic-multi-period setting of 2E-CLRP has not been tackled yet. We further note that existing 2E-CLRP and most LRP modeling approaches implicitly assume that location and routing decisions are made simultaneously for the planning horizon, without considering the hierarchical structure of the strategic problem that we stress here. Laporte [33] shows that the LRP is NP-hard. Thus, the 2E-CLRP inherits the same NP-hardness property from LRP. When considering uncertainty, the 2E-CLRP is an NP-hard stochastic combinatorial optimization problem. However, a few exact methods and metaheuristics proposed in the literature are designed for deterministic-static setting [20]. This justifies the development of advanced exact solution approaches to solve realistic-size instances of the problem. Decomposition methods such as L-shaped methods [62, 11] and Benders decomposition [10] are crucial to solve the two-stage stochastic programs.

The contribution of this paper is threefold. Firstly, we provide a more precise definition of the 2E-SM-CLRP under uncertain and time-varying demand and cost. The problem is casted as a two-level organizational decision process: location and capacity decisions are made on a yearly basis, whereas routing decisions are made on a daily basis in response to the customer orders received. This temporal hierarchy gives rise to a hierarchical decision problem and makes it necessary to use a stochastic and multi-period modeling approach. More precisely, the decision process aims to decide at each design period on opening, operating and closing of WPs and DPs, as well as the capacity allocated to links between platforms. In the second level, the goal is to periodically build routes that visit customers using a vehicle routed from an operating DP – see Figure 1 for an illustration. The objective is to minimize the total expected cost based on strategic and operational cost components. Secondly, we introduce a formulation of the 2E-SM-CLRP as a two-stage stochastic program with recourse. The scenario-based approach relies on a set of multi-period scenarios generated with a Monte-Carlo approach. The location and capacity decisions are taken here-and-now for the set of design periods considered. Second-stage decisions consist in building daily routes in the second echelon once customer orders are revealed, replicated for high number of scenarios. The two-stage stochastic formulation reduces the combinatorial complexity of the multi-stage process. However, solving 2E-SM-CLRP is still challenging due to the presence of multiple design periods in the first stage, in addition to the integer recourse problem [13, 36, 1]. As a third contribution, we propose an exact approach to solve realistic-size instances of the 2E-SM-CLRP. The proposed approach is based on the Benders decomposition [10] and the sample average approximation (SAA) [57]. It first fixes the operating WPs and DPs as well as the capacities allocated to links between platforms by solving the Benders master problem. Then, the resulting subproblem is a capacitated vehicle-routing problem with capacitated multi-depot (CVRP-CMD), which is a harder variant of the uncapacitated case. The CVRP-CMD is formulated as a set partitioning model strengthened by a lower bound on the number of vehicles obtained from the solution of a bin packing problem in preprocessing. Then, it is decomposed by period and by scenario. These latter are solved in parallel using the state-of-art branch-cut-and-price algorithm of Sadykov et al. [52]. Subproblem solutions are used to generate standard Benders cuts as well as combinatorial Benders cuts in order to converge to the optimal solution of the 2E-SM-CLRP. Extensive computational experiments on a large set of instances, emphasize the performance of the proposed algorithm on solving small-scale and mid-scale instances optimally, and on getting good lower bounds for large-scale instances with up to 50 customers and 25 demand scenarios under a 5-year planning horizon. Finally, we share the insights we derived from the computational experiment about the impact of the stochastic and multi-period settings on the 2E-CLRP.

The reminder of this paper is organized as follows. Section 2 briefly surveys the related work on the 2E-CLRP under stochastic and multi-period settings. Section 3 introduces the mathematical formulation. Section 4 presents the proposed exact solution approach. The computational results are presented and analyzed in Section 5. Section 6 concludes the study and outlines future research avenues.

## 2. Related works

As mentioned in the introduction, the literature on the 2E-CLRP is scarce at best. Therefore, in this section, we include the contributions on problems related to the 2E-CLRP.

The two-echelon vehicle-routing problem (2E-VRP) is a particular case of the 2E-CLRP, in which the location of all WPs and DPs is known in advance, platforms do not have capacities and they can be used freely without inducing a setup cost. Moreover, generally, a single main WP is considered in the upper level of the 2E-VRP. Several exact

methods [44, 45, 7] and heuristics [18, 28, 12, 65] have been developed in the literature. To the best of our knowledge, the best performing heuristics are the large neighbourhood search (LNS) heuristic proposed by Breunig et al. [12] and the metaheuristic proposed by Wang et al. [65] for the 2E-VRP with environmental considerations. A well performing exact algorithm is presented in [7]. As for the stochastic variant, Wang et al. [64] is the first to propose a genetic algorithm for 2E-VRP with stochastic demand. However, as far as we know, no previous study has considered both stochastic and multi-period features in 2E-VRP. For further details, interested readers are referred to a recent survey by Cuda et al. [20].

The capacitated location-routing problem (CLRP) is another related class of problems in which the location of main warehouses is known in advance and the cost between WPs and DPs are neglected. This problem combines the multi-depot vehicle-routing problem and the facility location problem. Several studies focus on the LRP and its variants. Proposed exact methods [5, 8, 14, 15] and heuristics [16, 27, 47, 49] are mostly to solve the problem in deterministic setting. However, some work study stochastic cases as well [35, 58, 2, 31]. Belenguer et al. [8] introduce a two-index vehicle-flow formulation strengthened with several families of valid inequalities for the CLRP which solved by a branch-and-cut algorithm. Contardo et al. [14] present three new flow formulations which are used to derive new valid inequalities. The authors also propose new improved separation routines for the inequalities introduced in [8]. Baldacci et al. [5] introduce a set partitioning formulation for the problem which is strengthened with new families of valid inequalities. Contardo et al. [15] strengthen the set partitioning formulation with new valid inequalities and propose an exact algorithm based on cut-and-column generation. Prins et al. [49] develop a greedy randomized adaptive search procedure (GRASP). Pirkwieser and Raidl [47] introduce the first hybrid metaheuristic for the CLRP combining the variable neighborhood search (VNS) and integer-linear programming techniques. Hemmelmayr et al. [28] present an ALNS for the 2E-CVRP and also test it on the CLRP instances. Finally, Contardo et al. [16] introduce a hybrid metaheuristic combining a GRASP with integer programming methods based on column generation which provides better results compared to previous methods.

Furthermore, the multi-period feature is also considered in some LRP models. Laporte and Dejax [34] examine a multi-period uncapacitated LRP (ULRP) with capacitated vehicles. Albareda-Sambola et al. [3] consider the multi-period ULRP with decoupled time scales, in which the routing decisions and the location decisions follow two different time scales. Stochastic setting is also tackled in the ULRP by Laporte et al. [35] and Albareda-Sambola et al. [2]. In the considered stochastic model, the depot locations and a priori routes must be specified in the first-stage, and second-stage recourse decisions deal with first-stage failures. Shen [58] proposes a stochastic LRP model based on routing cost estimations. Klibi et al. [31] examine the stochastic multi-period location transportation problem (SMLTP) where distribution centers are uncapacitated. The location and mission of depots must be fixed at the beginning of the planning horizon, but transportation decisions are made on a multi-period daily basis as a response to the uncertain customer demand. The authors formulate the SMLTP as a two-stage stochastic program with recourse, and solve it with a hierarchical heuristic approach based on SAA method which introduced by Shapiro [56] and has been successfully applied in [54] and [55].

Our review points to the literature's shortcomings in addressing the stochastic and multi-period versions of 2E-CLRP. It also demonstrates the lack of exact methods which deal with the stochastic version of this novel problem.

# 3. Mathematical formulation

In our problem 2E-SM-CLRP, we consider a long-term planning horizon $\mathcal{T}$ that covers a set of successive design planning periods $\mathcal{T} = \{1, \ldots, T\}$. Such periods are defined in accordance with the evolution of the uncertain customer demand over time (typically a year). Each planning period encompasses a set of operational periods represented generally in a discrete way with typical business days. Under uncertainty, the routing decisions depend on the actual realization of the demand at each period $t$. Thus, each realization defines a demand scenario $\omega$ representing a typical day of delivery which has a probability of occurrence $p(\omega)$. All potential scenarios characterize the set of demand scenarios $\Omega_t$ modeling the uncertainty behavior of customer demand at period $t$. Therefore, the set of all scenarios is $\Omega = \cup_t \Omega_t$.

The 2E-SM-CLRP is defined on a graph with three disjoint sets of nodes – those representing the potential locations for warehouse platforms (WPs), $\mathcal{P} = \{p\}$, those for the potential locations for distribution platforms (DPs), $\mathcal{L} = \{l\}$, and those for the customers, $\mathcal{J} = \{j\}$. WPs and DPs can be opened (started), kept operating or closed at any planning period with a time-varying fixed cost – i.e., respectively, $fw^s_{pt}$, $fw_{pt}$, $fw^c_{pt}$ for WP and $f^s_{lt}$, $f_{lt}$, $f^c_{lt}$ for DP. Each WP $p$ (respectively DP $l$) has a limited capacity $C_p$ (respectively $C_l$). Additionally, each customer $j$ has an uncertain demand $d^{t\omega}_j$ at period $t$ under scenario $\omega$.

At the first echelon, we consider an undirected bipartite graph $\mathcal{G}^1 = (\mathcal{V}^1, \mathcal{E}^1)$, with the vertex set $\mathcal{V}^1 = \mathcal{P} \cup \mathcal{L}$, and the edge set $\mathcal{E}^1 = \{(p, l) : p \in \mathcal{P}, l \in \mathcal{L}\}$ representing the WPs and DPs, and the links in between. These links

help to calibrate the DPs throughput. To each link we can assign one or several full truckloads, each of which has a capacity $Q^1_{lp}$ and a fixed cost $h_{lpt}$. Moreover, multi-sourcing strategy is allowed in the first echelon – i.e., each DP can be supplied from more than one operating WP – while respecting the capacity limitations. At the second echelon, an undirected graph $\mathcal{G}^2 = (\mathcal{V}^2, \mathcal{E}^2)$ is defined where $\mathcal{V}^2 = \mathcal{L} \cup \mathcal{J}$, and $\mathcal{E}^2 = \{(i,j) : i,j \in \mathcal{V}^2,\ j \notin \mathcal{L}\}$ representing the DPs and customers and the links in between. Note that no lateral transshipment between DPs is performed – i.e., there are no direct edges between DPs. A routing cost $c^t_{ij}$ is associated with each edge $(i,j) \in \mathcal{E}^2$ at period $t$ in the second echelon.

We consider an unlimited set $\mathcal{K}$ of identical vehicles with capacity $Q^2$ used to visit customers in the second echelon, where $Q^2 < Q^1_{lp}$. If used, a fixed cost is paid for each vehicle for which we assign a route in the second echelon. We assume that this cost is already incorporated into the routing cost in the following way. The cost $c^t_{ij}$ of each edge $(i,j) \in \mathcal{E}^2$ adjacent to a DP – i.e., those representing the departures from and arrivals at the DPs – is increased by the half of the fixed vehicle cost for each $t$.

The proposed model decides the opening, operating, and closing periods of each WP and DP, as well as the number of full truckloads assigned to each link $(p,l) \in \mathcal{E}^1$ thus defining the capacity allocated to DPs. In the second-stage, the goal is to build vehicle routes so that each customer is visited exactly once in each period and each scenario. The quantity delivered to customers from each operating DP under each scenario is less or equal to the capacity assigned to that DP from WPs. The objective is to minimize the total expected cost by minimizing the sum of the expected transportation cost and the design cost (facility location and capacity allocation).

The 2E-SM-CLRP is formulated as follows. At the first-stage, let $y^+_{pt}$, $y_{pt}$, and $y^-_{pt}$ be binary variables which take the value 1 if WP $p \in \mathcal{P}$ is selected for opening, operating and closing in period $t \in \mathcal{T}$. In a similar fashion, we define $z^+_{lt}$, $z_{lt}$, and $z^-_{lt}$ for each DP $l \in \mathcal{L}$. Let $x_{lpt}$ be an integer variable denoting the number of full truckloads assigned from WP $p$ to DP $l$ in period $t$.

Given a fixed first-stage design solution, the second-stage problem is modeled using a set partitioning formulation [61]. Let us denote by $\mathcal{R}^{t\omega}_l$ the set of all routes starting and ending at an operating DP $l$ satisfying capacity constraints for period $t$ under scenario $\omega \in \Omega_t$, and let $\mathcal{R} = \cup_{t\in\mathcal{T}} \cup_{\omega\in\Omega_t} \cup_{l\in\mathcal{L}} \mathcal{R}^{t\omega}_l$. Note that a route $r \in \mathcal{R}$ is not necessarily elementary, i.e. it can visit a client more than once. Let $\psi^r_{ij}$ denote the number of times edge $(i,j)$ participates in route $r \in \mathcal{R}$, and $\xi^r_j$ the number of times customer $j$ is visited in route $r \in \mathcal{R}$ ($\xi^r_j = \sum_{i\in\mathcal{J}|(i,j)\in\mathcal{E}^2} \psi^r_{ij}$). Then $\sum_{j\in\mathcal{J}} d^{t\omega}_j \xi^r_j \leqslant Q^2$ should hold for every $r \in \mathcal{R}^{t\omega}_l$. Cost $c^t_r$ of route $r \in \mathcal{R}^{t\omega}_l$ is calculated as $c^t_r = \sum_{(i,j)\in\mathcal{E}^2} \psi^r_{ij} c^t_{ij}$.

Let $\lambda^{t\omega}_{lr}$ be a binary variable indicating whether a route $r \in \mathcal{R}^{t\omega}_l$ is selected in the optimal solution. The two-stage stochastic integer program with recourse then can be written as:

$$\min \sum_{t\in\mathcal{T}} \sum_{p\in\mathcal{P}} (fw^s_{pt}\, y^+_{pt} + fw_{pt}\, y_{pt} + fw^c_{pt}\, y^-_{pt}) + \sum_{t\in\mathcal{T}} \sum_{l\in\mathcal{L}} (f^s_{lt}\, z^+_{lt} + f_{lt}\, z_{lt} + f^c_{lt}\, z^-_{lt}) + \sum_{t\in\mathcal{T}} \sum_{p\in\mathcal{P}} \sum_{l\in\mathcal{L}} h_{lpt} x_{lpt} + \sum_{t\in\mathcal{T}} \mathbb{E}_{\Omega_t}[\phi_{t\omega}(x)] \tag{1}$$

$$\text{s.t.} \quad \sum_{l\in\mathcal{L}} Q^1_{lp} x_{lpt} \leqslant C_p\, y_{pt} \qquad \forall p,t \tag{2}$$

$$\sum_{p\in\mathcal{P}} Q^1_{lp} x_{lpt} \leqslant C_l\, z_{lt} \qquad \forall l,t \tag{3}$$

$$y_{pt} - y_{pt-1} \leqslant y^+_{pt} \qquad \forall p \in \mathcal{P}, t \in \mathcal{T} \tag{4}$$

$$z_{lt} - z_{lt-1} \leqslant z^+_{lt} \qquad \forall l \in \mathcal{L}, t \in \mathcal{T} \tag{5}$$

$$y_{pt-1} - y_{pt} \leqslant y^-_{pt} \qquad \forall p \in \mathcal{P}, t \in \mathcal{T} \tag{6}$$

$$z_{lt-1} - z_{lt} \leqslant z^-_{lt} \qquad \forall l \in \mathcal{L}, t \in \mathcal{T} \tag{7}$$

$$\sum_t y^+_{pt} \leqslant 1 \qquad \forall p \in \mathcal{P} \tag{8}$$

$$\sum_t y^-_{pt} \leqslant 1 \qquad \forall p \in \mathcal{P} \tag{9}$$

$$\sum_t z^+_{lt} \leqslant 1 \qquad \forall l \in \mathcal{L} \tag{10}$$

$$\sum_t z^-_{lt} \leqslant 1 \qquad \forall l \in \mathcal{L} \tag{11}$$

$$x_{lpt} \in \mathbb{N} \qquad \forall l \in \mathcal{L}, p \in \mathcal{P}, t \in \mathcal{T} \tag{12}$$

$$y^+_{pt}, y_{pt}, y^-_{pt} \in \{0,1\} \qquad \forall p \in \mathcal{P}, t \in \mathcal{T} \tag{13}$$

$$z^+_{lt}, z_{lt}, z^-_{lt} \in \{0,1\} \qquad \forall l \in \mathcal{L}, t \in \mathcal{T} \tag{14}$$

where $\phi^{t\omega}(x)$ is the solution of the recourse problem:

$$(\text{SPF}_{t\omega}) \quad \phi_{t\omega}(x) = \min \sum_{l\in\mathcal{L}} \sum_{r\in\mathcal{R}_l^{t\omega}} c_r^t \lambda_{lr}^{t\omega} \tag{15}$$

$$\text{S. t.} \quad \sum_{l\in\mathcal{L}} \sum_{r\in\mathcal{R}_l^{t\omega})} \xi_j^r \lambda_{lr}^{t\omega} = 1 \qquad \forall j \in \mathcal{J} \tag{16}$$

$$\sum_{r\in\mathcal{R}_l^{t\omega}} \left( \sum_{j\in\mathcal{J}} d_j^{t\omega} \xi_j^r \right) \lambda_{lr}^{t\omega} \leqslant \sum_{p\in\mathcal{P}} Q_{lp}^1 x_{lpt} \qquad \forall l \in \mathcal{L} \tag{17}$$

$$\sum_{l\in\mathcal{L}} \sum_{r\in\mathcal{R}_l^{t\omega}} \lambda_{lr}^{t\omega} \geqslant \Gamma^{t\omega} \tag{18}$$

$$\lambda_{lr}^{t\omega} \in \{0,1\} \qquad \forall l \in \mathcal{L}, r \in \mathcal{R}_l^{t\omega} \tag{19}$$

The objective function (1) minimizes the sum of the first-stage costs and the expected second-stage costs. The first-stage cost is the sum of the opening, operating, and closing costs of the WPs and DPs, and the capacity cost induced by the number of truckloads allocated to DPs from WPs. Constraints (2) and (3) guarantee the capacity restriction at operating WPs and DPs, respectively. Constraints (4) and (5) track the operating status of the WPs and DPs from one period to the next and mark the period of their opening. In a similar vein, constraints (6) and (7) manage the closing status of WPs and DPs, respectively. Constraints (8)–(11) specify that each platform is opened or closed at most once during the planning horizon. Constraints (12)–(14) describe the domain of the first-stage variables.

The second-stage objective function (15) minimizes the routing cost and the fixed cost for using vehicles. Constraints (16) ensure that each customer is served exactly once. Constraints (17) are the depot capacity inequalities. They guarantee that the demand satisfied from an operating DP will not exceed its throughput capacity. Inequalities (18) are added to strengthen the linear relaxation of (SPF) by imposing a lower bound $\Gamma^{t\omega}$ on the number of vehicles required to serve customer demand in period $t$ under scenario $\omega$. This lower bound is obtained through the solution of a bin packing problem (BPP) in which the aim is to pack a given set of items having different weights into a minimum number of equal-sized bins [38]. In this model, the set of items represents the set of customers $\mathcal{J}$ where each item has a weight $d_j^{t\omega}$ – i.e. the customer demand – and the bin capacity is the vehicle capacity $Q^2$. More precisely, $\Gamma^{t\omega}$ is the value of the linear relaxation of (BPP) obtained for period $t$ and scenario $\omega$.

# 4. Benders approach

In this section, we present the proposed Benders decomposition algorithm to solve the 2E-SM-CLRP where the integer recourse is handled through two steps iteratively. The algorithm separates the problem into a Benders master problem (MP) and a number of Benders subproblems, which are easier to solve than the original problem. By using linear programming duality, all subproblem variables are projected out and the relaxed MP contains only the remaining master variables and artificial variables representing the lower bounds on the cost of each subproblem. In the first-stage, location (WPs and DPs) and capacity assignment decisions are taken by solving the Benders master problem. When these first-stage decisions are fixed in the original problem, the resulting subproblem is a capacitated vehicle-routing problem with capacitated multi-depot (CVRP-CMD) that can be decomposed by period and by scenario. However, solving these subproblems as an integer program does not produce dual values to generate standard Benders cuts. In order to generate valid Benders cuts, we iteratively tackle the second-stage integer program. The main steps of our solution approach are summarized in Figure 2. As a preprocessing step, we solve the linear relaxation of a bin packing problem (BPP) for each period and each scenario through column generation. Rounded up values of the obtained bounds are then introduced to the Benders subproblems as a lower bound on the number of vehicles required for each period and each scenario. Further details on the BPP are given in Appendix A. Then, at each iteration of the Benders approach, a relaxed integer MP – which includes only the Benders cuts generated so far –, is optimally solved to obtain a valid dual bound and a first-stage solution. Using such fixed first-stage decisions (operating DPs and capacity assignment), we first relax the integrality restrictions in the Benders subproblems (i.e., CVRP-CMD). For each period and scenario, we solve the LP of the set partitioning formulation (SPF) (15)–(19) using the column generation approach to generate a Benders optimality cuts from the dual solutions. These cuts are then added to the MP. If there are no new Benders optimality cuts, the integer subproblems are then solved using the branch-cut-and-price algorithm of Sadykov et al. [52]. This algorithm is demonstrated to be the best performing exact approach for many classical variants of the vehicle routing problem. The expected total cost of the integer feasible solutions of subproblems yields a primal bound for the 2E-SM-CLRP. If the gap is still larger than $\epsilon$, combinatorial

Benders cuts are added to the MP to eliminate the current master solution. This process is repeated until an optimal solution is found or the relative gap is smaller than a given $\epsilon$ threshold.

In the following, we first describe the Benders master problem (MP). Then, we present the Benders subproblems and the generated Benders cuts. Finally, we give a complete description of the Benders algorithm used to solve the 2E-SM-CLRP.

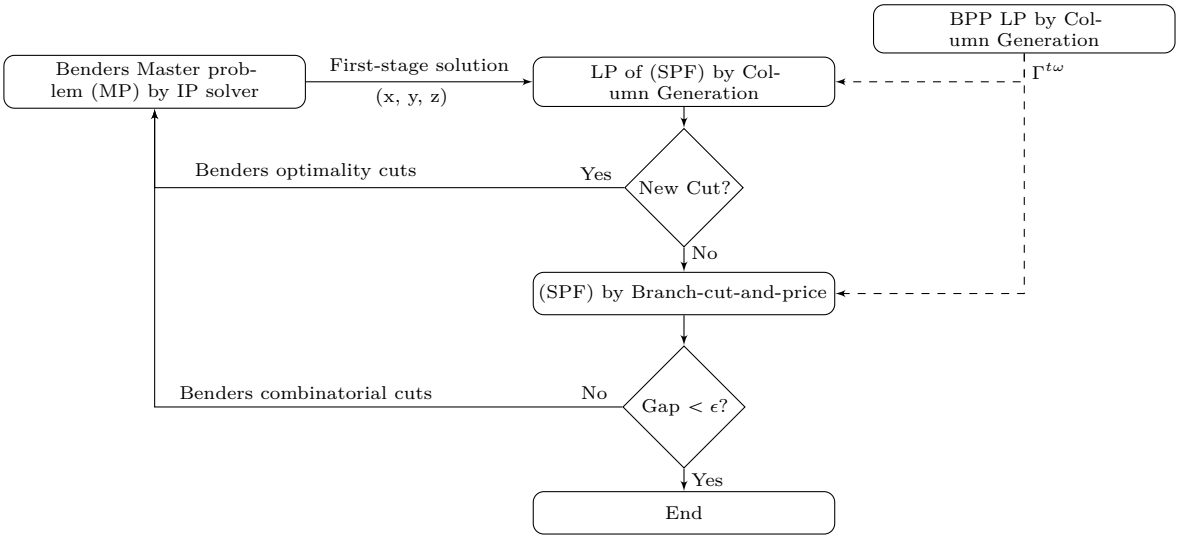


Figure 2: Main steps of our solution approach

## 4.1 Benders master problem

The Benders master problem (MP) includes the first-stage decisions: location decisions for WPs and DPs and capacity assignment decisions. Introducing an additional variable $\theta_{t\omega}$ representing the total second-stage decisions cost for period $t$ and scenario $\omega$, we then formulate the MP as:

$$\text{(MP)}\ \min \sum_{t\in\mathcal{T}}\sum_{p\in\mathcal{P}}(fw_{pt}\,y_{pt}+fw^s_{pt}\,y^+_{pt}+fw^c_{pt}\,y^-_{pt})+\sum_{t\in\mathcal{T}}\sum_{l\in\mathcal{L}}(f_{lt}\,z_{lt}+f^s_{lt}\,z^+_{lt}+f^c_{lt}\,z^-_{lt})+\sum_{t\in\mathcal{T}}\sum_{p\in\mathcal{P}}\sum_{l\in\mathcal{L}}h_{lpt}x_{lpt}+\sum_{t\in\mathcal{T}}\sum_{\omega\in\Omega}p(\omega)\theta_{t\omega} \tag{20}$$

$$\text{s.t.} \quad (2)-(14)$$

$$\theta_{t\omega}\geqslant 0 \quad \forall t\in\mathcal{T},\omega\in\Omega \tag{21}$$

It is worth noting that relaxed MP contains only the integer design variables and $|\mathcal{T}|\times|\Omega_t|$ additional continuous variables at the beginning. Benders optimality cuts and combinatorial cuts are added to the model iteratively after solving subproblems.

In each iteration $k$, the optimal solution of the master problem provides a dual bound ($v^k_{MP}$) for the 2E-SM-CLRP. We define $v^k_{design}=\sum_{t\in\mathcal{T}}\sum_{p\in\mathcal{P}}(fw_{pt}y_{pt}+fw^s_{pt}y^+_{pt}+fw^c_{pt}y^-_{pt})+\sum_{t\in\mathcal{T}}\sum_{l\in\mathcal{L}}(f_{lt}z_{lt}+f^s_{lt}z^+_{lt}+f^c_{lt}z^-_{lt})+\sum_{t\in\mathcal{T}}\sum_{p\in\mathcal{P}}\sum_{l\in\mathcal{L}}h_{lpt}x_{lpt}$ as the cost value of the design variables.

## 4.2 Benders subproblems

For a fixed set of operating DPs and a capacity assignment, the recourse problem can be decomposed into $|T|\times|\Omega|$ subproblems, which are CVRP-CMD problems, one for each period $t\in\mathcal{T}$ and each scenario $\omega\in\Omega_t$.

Let $\bar{x}^k$ denote the vector of fixed variables in iteration $k$. Solution values $\phi_{t\omega}(\bar{x}^k)$ for the subproblems can be used to compute the expected total cost $\phi(\bar{x}^k)$ of the second-stage decisions: $\phi(\bar{x}^k)=\sum_{t\in\mathcal{T}}\sum_{\omega\in\Omega_t}p(\omega)\phi_{t\omega}(\bar{x}^k)$.

### 4.2.1 Generating Benders optimality cuts

As pointed out at the beginning of Section (4), we start by solving the linear relaxation (SPLP$_{t\omega}$) of the set partitioning formulation (SPF$_{t\omega}$) for all periods $t\in\mathcal{T}$ and for all scenarios $\omega\in\Omega_t$. Due to the exponential size of $\mathcal{R}^{t\omega}_l$,

every ($\text{SPLP}_{t\omega}$) is solved using column generation. It is an iterative approach in which in every iteration a subset of variables $\lambda$ is considered, and a restricted set-partitioning linear program ($\text{RSPLP}_{t\omega}$) is solved. Let ($\tau^{t\omega}$, $\rho^{t\omega}$, $\iota^{t\omega}$) be an optimal dual solution of ($\text{RSPLP}_{t\omega}$), corresponding to constraints (16), (17), and (18). To determine whether this dual solution is optimal for ($\text{SPLP}_{t\omega}$), a pricing problem is solved. The pricing problem searches for a route $r \in \mathcal{R}_l^{t\omega}$, $l \in \mathcal{L}$, with a negative reduced cost. If such routes are found, the corresponding variables $\lambda$ are added to ($\text{RSPLP}_{t\omega}$), and we pass to the next iteration. The pricing problem is decomposed into $|\mathcal{L}|$ problems, one for each DP. Reduced cost $\hat{c}_{lr}^{t\omega}$ of a route $r \in \mathcal{R}_l^{t\omega}$ is computed as

$$\hat{c}_{lr}^{t\omega} = c_r^t - \sum_{j \in \mathcal{J}} \tau_j^{t\omega} \xi_j^r + \left( \sum_{j \in \mathcal{J}} d_j^{t\omega} \xi_j^r \right) \rho_l^{t\omega} - \iota^{t\omega}. \tag{22}$$

By replacing $\xi$ by $\psi$ and removing the constant part in (22), the pricing problem for ($\text{RSPLP}_{t\omega}$) and DP $l \in \mathcal{L}$ can be formulated as

$$\min_{r \in \mathcal{R}_l^{t\omega}} \hat{c}_{lr}^{t\omega} = \min_{r \in \mathcal{R}_l^{t\omega}} \sum_{(i,j) \in \mathcal{E}^2} (c_{ij}^t - \tau_j^{t\omega}) \psi_{ij}^r. \tag{23}$$

Each pricing problem is a Resource Constrained Shortest Path (RCSP) problem. The aim here is to find a minimum cost path linking a source vertex to a sink vertex that satisfy the capacity constraint. This problem can be efficiently treated using dynamic programming labeling algorithms [29, 51]. In this study, we use the bucket graph based labeling algorithm of Sadykov et al. [52].

Note that set $\mathcal{R}_l^{t\omega}$ of routes can be restricted to only elementary ones (passing by each customer at most once) without eliminating any feasible solution of the 2E-SM-CLRP. Relaxation of ($\text{SPLP}_{t\omega}$) is tighter in this case. However, considering only elementary routes in the pricing can render it hard to be solved. Instead, we use *ng*-route relaxation [6], known to have a good trade-off between formulation strength and pricing difficulty. An *ng*-route can only revisit a customer $i$ if it first passes by a customer $j$ such that $i$ is not in a pre-defined neighbourhood of $j$. In many instances, reasonably small neighborhoods (for example, of size 8) already provide tight bounds that are close to those that would be obtained by pricing elementary routes [48].

To insure the feasibility of each ($\text{SPLP}_{t\omega}$), we add slack variables to constraints (16)–(18). We set the coefficients for these variables in the objective function large enough, so that the second-stage decisions are feasible for every period and every scenario in the final solution obtained for the 2E-SM-CLRP.

Dual solution ($\bar{\tau}^{t\omega}$, $\bar{\rho}^{t\omega}$, $\bar{\iota}^{t\omega}$) is optimal for ($\text{SPLP}_{t\omega}$) if no route with negative reduced cost if found after solving the pricing problem. Thus this solution is feasible for the dual of ($\text{SPLP}_{t\omega}$), and by linear programming duality, the following inequality is valid for the (MP):

$$\theta_{t\omega} + \sum_{l \in \mathcal{L}} \sum_{p \in \mathcal{P}} Q_{lp}^1 \bar{\rho}_l^{t\omega} x_{lpt} \geqslant \sum_{j \in \mathcal{J}} \bar{\tau}_j^{t\omega} + \Gamma^{t\omega} \bar{\iota}^{t\omega} \tag{24}$$

In iteration $k$ of our Benders algorithm, we solve ($\text{SPLP}_{t\omega}$) for all periods $t$ and all scenarios $\omega$. All violated inequalities of form (24) are then added to (MP). These constraints are referred to as Benders optimality cuts.

#### 4.2.2 Generating combinatorial Benders cuts

If none of inequalities (24) is violated, formulations ($\text{SPF}_{t\omega}$) for each period $t$ and each scenario $\omega \in \Omega_t$ are then solved using the state-of-the-art branch-cut-and-price algorithm of Sadykov et al. [52].

The branch-cut-and-price algorithm is based on a combination of column generation, cut generation and branching. For each node of the branch-and-bound, the lower bound on the optimal cost is computed by solving the problem ($\text{SPLP}_{t\omega}$) enhanced with Rounded Capacity Cuts (RCC) [37] and limited memory Rank-1 Cuts (R1C) [30, 43] using column generation as described in Section 4.2.1. Column generation convergence is improved with the automatic dual pricing stabilization technique proposed in [46]. After each convergence, the algorithm performs a bucket arc elimination procedure based on the reduced costs [52] Then, a bi-directional enumeration procedure [4] is called to try to generate all improving elementary routes with reduced cost smaller than the current primal-dual gap. If the pricing problem corresponding to a DP $l \in \mathcal{L}$ is successfully enumerated, the current ($\text{RSPLP}_{t\omega}$) is updated by excluding non-elementary columns corresponding to routes in $\mathcal{R}_l^{t\omega}$. This pricing problem is then solved by inspection. When pricing problems for all DPs $l \in \mathcal{L}$ are enumerated and the total number of routes is small, the node is finished by a MIP solver.

On the other hand, if there exists at least one non-enumerated pricing problem that is too time consuming to solve and the tailing off condition for cut generation is reached, branching is performed. Three different branching strategies are used, they can be expressed as constraints over the following aggregated variables:

- branching on the number of vehicles used from a DP $l$: $\sum_{r\in\mathcal{R}_l^{t\omega}}\sum_{j\in\mathcal{J}}\frac{1}{2}\psi_{lj}^r\lambda_{lr}^{t\omega},\ \forall l\in\mathcal{L}$,
- branching on the assignment of a customer $j\in\mathcal{J}$ to an operating DP $l$: $\sum_{r\in\mathcal{R}_l^{t\omega}}\xi^j\lambda_{lr}^{t\omega},\ \forall j\in\mathcal{J},\ l\in\mathcal{L}$,
- branching on the edges of the original graph:$\sum_{l\in\mathcal{L}}\sum_{r\in\mathcal{R}_l^{t\omega}}\psi_{ij}^r\lambda_{lr}^{t\omega},\ (i,j)\in\mathcal{E}^2$.

Branching variables are selected according to a sophisticated hierarchical strong branching procedure, inspired from [43].

Note that $\phi_{t\omega}(\bar{x}^k)$ is the solution value of ($\text{SPF}_{t\omega}$) and the branch-cut-and-price algorithm finds values $\underline{\theta}_{t\omega}^k$ and $\hat{\theta}_{t\omega}^k$, which are lower and upper bounds on the value $\phi_{t\omega}(\bar{x}^k)$. If ($\text{SPF}_{t\omega}$) is solved to optimality, both values coincide. After solving all problems ($\text{SPF}_{t\omega}$), primal bound on the solution value of the 2E-SM-CLRP can be computed as

$$v_{design}^k+\sum_{t\in\mathcal{T}}\sum_{\omega\in\Omega_t}p(\omega)\hat{\theta}_{t\omega}^k. \tag{25}$$

If the optimality gap – i.e., difference between dual bound $v_{MP}^k$ and primal bound (25) – is sufficiently small, the algorithm is stopped. Otherwise, combinatorial Benders cuts are generated, which we describe in the following.

The intuition behind the combinatorial cuts is the following. Given period $t\in\mathcal{T}$, if for every $l\in\mathcal{L}$ the capacity of DP $l$ induced by the first-stage decisions is not larger than $\sum_{p\in\mathcal{P}}Q_{lp}^1\bar{x}_{lpt}^k$, then for any scenario $\omega\in\Omega_t$ the value $\theta_{t\omega}$ of the second-stage decisions cannot be smaller than $\underline{\theta}_{t\omega}^k$. This idea can be represented as follows:

$$\forall t\in\mathcal{T}:\quad\begin{cases}\theta_{t\omega}\geqslant\underline{\theta}_{t\omega}^k,\forall\omega\in\Omega_t, & \text{if }\sum_{p\in\mathcal{P}}Q_{lp}^1x_{lpt}\leqslant\sum_{p\in\mathcal{P}}Q_{lp}^1\bar{x}_{lpt}^k,\forall l\in\mathcal{L},\\ \theta_{t\omega}\geqslant 0,\forall\omega\in\Omega_t, & \text{otherwise.}\end{cases} \tag{26}$$

In order to linearize conditions (26), additional variables are introduced. We define $a_t^k$ as a non-negative variable representing the maximum capacity increase of a DP in period $t$ in comparison with the fixed DP capacities of iteration $k$:

$$a_t^k=\max\left(0,\ \max_{l\in\mathcal{L}}\left(\sum_{p\in\mathcal{P}}Q_{lp}^1x_{lpt}-\sum_{p\in\mathcal{P}}Q_{lp}^1\bar{x}_{lpt}^k\right)\right) \tag{27}$$

Let also $g_t^k$ be a binary variable equal to 1 if and only if the value of $a_t^k$ is strictly positive. In addition, we define binary variables $b_{lt}^k$ and $b_{0t}^k$ involved in the linearisation of expression (27). Let $M'$ be a value which is larger than any possible value variables $a$ can take – i.e., $M'\geqslant C_l$, $l\in\mathcal{L}$. The combinatorial Benders cuts are then formulated as:

$$a_t^k\leqslant M'g_t^k\qquad\forall t\in\mathcal{T} \tag{28}$$
$$g_t^k\leqslant a_t^k\qquad\forall t \tag{29}$$
$$\theta_{t\omega}\geqslant\underline{\theta}_{t\omega}^k(1-g_t^k)\qquad\forall t\in\mathcal{T},\omega\in\Omega_t \tag{30}$$
$$\sum_{p\in\mathcal{P}}Q_{lp}^1x_{lpt}-\sum_{p\in\mathcal{P}}Q_{lp}^1\bar{x}_{lpt}^k\leqslant a_t^k\qquad\forall t\in\mathcal{T},l\in\mathcal{L} \tag{31}$$
$$a_t^k\leqslant\sum_{p\in\mathcal{P}}Q_{lp}^1x_{lpt}-\sum_{p\in\mathcal{P}}Q_{lp}^1\bar{x}_{lpt}^k+M'(1-b_{lt}^k)\qquad\forall t\in\mathcal{T},l\in\mathcal{L} \tag{32}$$
$$a_t^k\leqslant M'(1-b_{0t}^k)\qquad\forall t\in\mathcal{T} \tag{33}$$
$$b_{0t}^k+\sum_l b_{lt}^k=1\qquad\forall t\in\mathcal{T} \tag{34}$$
$$a_t^k\in\mathbb{R}_+\qquad\forall t\in\mathcal{T} \tag{35}$$
$$b_{lt}^k,b_{0t}^k,g_t^k\in\{0,1\}\qquad\forall t\in\mathcal{T},l\in\mathcal{L} \tag{36}$$

Constraints (28) and (29) link the variables $a$ and $g$. Constraints (30) impose lower bounds on variables $\theta$ according to the first condition in (26). As for constraints (31)–(34), they express a linearization of the definition (27) of variables $a$.

**Algorithm 1** Benders approach for the 2E-SM-CLRP

$\epsilon$ is set to the maximum optimality gap
$ub \leftarrow \infty$, $lb \leftarrow -\infty$, $k \leftarrow 0$
**for all** $t \in \mathcal{T}$, $\omega \in \Omega_t$ **do**
  Solve the linear relaxation of the bin packing problem (BPP) to obtain $\Gamma^{t\omega}$
**end for**
**while** $(ub - lb)/ub > \epsilon$ **do**
  Solve the (MP) to obtain solution $(\bar{x}^k, \bar{\theta}^k)$ of value $v^k_{MP}$
  $lb \leftarrow \max\{lb, v^k_{MP}\}$
  $newCut \leftarrow false$
  **for all** $t \in \mathcal{T}$, $\omega \in \Omega_t$ **do**
    Solve ($\text{SPLP}_{t\omega}$) by column generation to obtain dual solution $(\bar{\tau}^{t\omega}, \bar{\rho}^{t\omega}, \bar{\iota}^{t\omega})$ of value $\phi^{LP}_{t\omega}(\bar{x}^k)$
    **if** $\bar{\theta}^k_{t\omega} < \phi^{LP}_{t\omega}(\bar{x}^k)$ **then**
      Add the Benders optimality cut (24) to the (MP)
      $newCut \leftarrow true$
    **end if**
  **end for**
  **if** $newCut = false$ **then**
    **for all** $t \in \mathcal{T}$, $\omega \in \Omega_t$ **do**
      Solve the ($\text{SPF}_{t\omega}$) by branch-cut-and-price to obtain lower bound $\underline{\theta}^k_{t\omega}$ and upper bound $\hat{\theta}^k_{t\omega}$
      **if** $\bar{\theta}^k_{t\omega} < \underline{\theta}^k_{t\omega}$ **then**
        Add combinatorial Benders cuts (28)–(36) to the (MP)
      **end if**
    **end for**
    $\phi(\bar{x}^k) \leftarrow \sum_{t\in\mathcal{T}} \sum_{\omega\in\Omega_t} p(\omega)\hat{\theta}_{t\omega}(\bar{x}^k)$
    $ub \leftarrow \min\{ub, v^k_{design} + \phi(\bar{x}^k)\}$
    **if** $\underline{\theta}^k_{t\omega} < \hat{\theta}^k_{t\omega}$ for some $t$, $\omega$ and no violated cuts (28)–(36) were added to the (MP) **then**
      **stop**
    **end if**
  **end if**
  $k \leftarrow k + 1$
**end while**

## 4.3 Overall algorithm

The complete description of the Benders approach is given in Algorithm 1.

We will now prove that our Benders approach converges to an optimum solution of the 2E-SM-CLRP under certain conditions.

**Proposition 1.** *Algorithm 1 finds an optimum solution to the 2E-SM-CLRP after a finite number of iterations if* $\epsilon = 0$ *and second-stage integer problems (*$\text{SPF}_{t\omega}$*) are solved to optimality at every iteration.*

*Proof.* The validity of Benders optimality cuts follows from the strong duality of linear programming. The validity of combinatorial Benders cuts follows from the fact that they follow a linearization of conditions (26).

The overall number of cuts is finite, as the number of different solutions $\bar{x}$ is finite. Therefore, there exists finite iteration $k$ such that solution $\bar{x}^k$ is the same as solution $\bar{x}^{k'}$ at some previous iteration $k' < k$. The lower bound in iteration $k$ is not smaller than $v^k_{design} + \sum_{t\in\mathcal{T}} \sum_{\omega\in\Omega_t} p(\omega)\bar{\theta}^k$. As all problems ($\text{SPF}_{t\omega}$) were solved to optimality in iteration $k'$, upper bound is not larger than $v^{k'}_{design} + \sum_{t\in\mathcal{T}} \sum_{\omega\in\Omega_t} p(\omega)\underline{\theta}^{k'}$.

As $\bar{x}^{k'} = \bar{x}^k$, we have $v^k_{design} = v^{k'}_{design}$. Also from the construction of combinatorial cuts, we have $\bar{\theta}^k \geqslant \underline{\theta}^{k'}$ for all periods $t$ and all scenarios $\omega$. Thus, the lower and upper bounds match in iteration $k$, and feasible solution obtained in iteration $k'$ is optimal for the 2E-SM-CLRP. □

The algorithm may stop before reaching predefined gap $\epsilon$ if the overall time limit is reached or if not all second-stage problems ($\text{SPF}_{t\omega}$) are solved to optimality. In this case, we are not guarantees to obtain a feasible solution. However, the results of our experiments below show that we were always able to obtain it in such cases.

Table 1: Test problems size

| $\|\mathcal{P}\|$ | 4 | | | | | | | | |
|---|---|---|---|---|---|---|---|---|---|
| $\|\mathcal{L}\|$ | 8 | | | 12 | | | 16 | | |
| $\|\mathcal{J}\|$ | 15 | 20 | 50 | 15 | 20 | 50 | 15 | 20 | 50 |

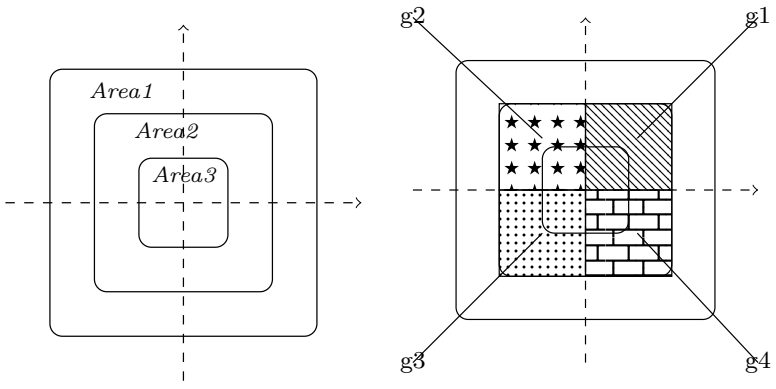


(a) The three urban area (b) Customers dispersion zones

Figure 3: Representation of two-echelon urban area

# 5. Computational results

In this section, we present our experimental results. First, we present the instances used in the experiments. Then, we report and discuss the obtained results.

Our approach is implemented in the C++ and compiled with GCC 5.3.0. BaPCod package [63] is used to handle the branch-cut-and-price framework. We use *CPLEX* 12.8.0 as the linear programming solver in column generation and as the integer programming solver for the set partitioning problem with enumerated columns as well as for the Benders master problem (MP). All tests are run on a cluster of 2 dodeca-core Haswell Intel Xeon E5-2680 v3 server running at 2.50 GHz with 128Go RAM. The OpenMP API [42] is used to solve the $|T| \times |\Omega_t|$ CVRP-CMD subproblems in parallel.

## 5.1 Test data

To test our approach, several 2E-SM-CLRP instances have been randomly generated based on the following attributes: the problem size, the network characteristics, the demand process, the cost structure as well as the capacity dimension. Problems of nine different sizes are tested as shown in Table 1. In each case, it is either the number of DPs ($|\mathcal{L}|$) or the number of customers ($|\mathcal{J}|$) that varies. The number of potential WPs ($|\mathcal{P}|$) is also provided. We mention that the sets of potential DPs given in instances with $|\mathcal{L}| = 8$ DPs and $|\mathcal{L}| = 12$ DPs are subsets of the large set with $|\mathcal{L}| = 16$ DPs. A 5-year planning horizon is considered, which is partitioned into 5 design periods – i.e., $|\mathcal{T}| = T = 5$.

Platforms and customers are realistically scattered in a geographic area within a concentric square of increasing size. We assume that the covered geographic territory is composed of three urban areas *Area1*, *Area2* and *Area3*, where *Area3* represents the central area. Figure 3(a) illustrates the partition of the three urban areas made in a way to scatter realistically the customers locations and the 2-echelon platforms. Coordinates of customers and platforms potential locations are randomly generated in the defined urban area using the following criteria. Customers are randomly located within *Area2* and *Area3*. $\alpha$ is the ratio of customers randomly located in *Area3* and $(1 - \alpha)$ is the ratio of customers within *Area2*. DPs are located within *Area2* and *Area3*. 20% of the total number of DPs is randomly located in the central *Area3*, and 80% of DPs are in *Area2*. WPs are randomly located within *Area1*. Depending on the ratio $\alpha$, two instance types are defined: I1 refers to concentric customers case where $\alpha = 0.8$ of customers are located within *Area3* and 20% in *Area2*. I2 corresponds to dispersed case where $\alpha = 0.6$.

Euclidean distances between nodes are computed, and two unit costs are defined to compute platform costs and transportation costs. Higher unit cost is attributed to DPs within *Area3* compared to the other areas. Two transportation costs configurations are tested: low transportation cost (LT) where the transportation cost represents 40% of the total network cost, and a high transportation cost (HT) where the trade-off is 60%. These ratios are

Table 2: Demand processes

| Demand process | Mean value | Trend |
|---|---|---|
| NIT | $\mu_{jt} = \mu_{jt-1}(1 + \delta_{z_j t})$ | $\delta_{z_j t} \in [0, 0.4]$ such that $\sum_{z_j t} \delta_{z_j t} = 0.4$ |
| NVT | $\mu_{jt} = \mu_{jt-1}(1 + \delta_{z_j t})$ | $\delta_{z_j t} \in [0, 0.9]$ such that $\sum_{z_j t} \delta_{z_j t} = 0.9$ |
| | $\mu_{jt} = \mu_{jt-1}(1 - \delta_{z_j t})$ | $\delta_{z_j t} \in [0, 0.4]$ |
| $\mu_{j0} \in [5, 25]$, $\frac{\sigma_{jt}}{\mu_{jt}} = 0.25$ | | |

determined based on some preliminary tests. At the second echelon, vehicle capacity is fixed to $Q^2 = 75$, and its fixed cost is $f = 600$ under the (LT) attribute and $f = 1300$ under (HT) attribute. The fixed WPs and DPs opening costs are generated, respectively in the ranges $fw_{pt} \in [14000, 25000]$ and $f_{lt} \in [7000, 10000]$ per location and period. An inflation factor is considered to reflect the increase of the cost of capital on a periodic basis with $r = 0.005$. The operating cost for both WPs and DPs is $fw^s_{pt} = 0.12 fw_{pt}$, and the closing cost $fw^c_{pt}$ is about $0.2 fw_{pt}$. Additionally, we define two capacity configurations: a tight level (TC) where $C_p$ and $C_l$ are uniformly generated in the intervals $[600, 900]$ and $[220, 400]$ respectively; and a large level (LC) in which WPs and DPs capacities are uniformly generated in the intervals $[850, 1400]$ and $[550, 800]$, respectively. The truckload capacities $Q^1_{lp}$ between WPs and DPs are generated in the interval $[150, 250]$.

Furthermore, we assume here, without loss of generality, that the demand scenario $d^{t\omega}_j$ of a customer $j$ in period $t$ follows the normal distribution with mean value $\mu_{jt}$ and standard deviation $\sigma_{jt}$. The customers are dispersed over four zones *g1, g2, g3* and *g4* within *Area2* and *Area3* as mentioned in Figure 3(b). For each zone $g$ and each period $t$, we define an inflation-deflation factor $\delta_{gt}$. Each customer mean demand $\mu_{jt}$ depends on the time-varying trend $\delta_{gt}$ and on its mean value at the previous period. The coefficient of variation ($\frac{\sigma_{jt}}{\mu_{jt}}$) is a fixed parameter for each customer over periods. Two time-varying trends are tested providing two demand processes. The normal distribution with an increasing trend (NIT) refers to a customer mean value that follows an increasing factor $\delta_{gt} \in [0, 0.4]$ such that $\sum_g \delta_{gt} = 0.4$. The second one is the normal distribution with a variable trend (NVT) where each customer mean demand varies according to an increasing trend $\delta_{gt} \in [0, 0.9]$ for periods $t = 1..3$ and then according to a decreasing trend for $t = 4, 5$. The values and ranges for all the parameters regarding to the demand process are given in Table 2. Combining all the elements above yields several problem instances. Each instance is denoted by a problem size $T$-$|\mathcal{P}|/|\mathcal{L}|/|\mathcal{J}|$-, a scenario sample size $N$ and a combination of customer dispersion (I1, I2), transportation attribute (LT, HT), capacity configuration (TC, LC) and the demand process (NIT, NVT).

## 5.2 Parameters

The Benders decomposition algorithm terminates when one of the following criteria is met: (i) the optimality gap between the upper and lower bounds is below an $\epsilon = 0.0005$ threshold – i.e., $(ub - lb)/ub < \epsilon$ – or (ii) the maximum time limit of 72 hours is reached. A time limit of 50 minutes is considered for each CVRP-CMD.

An important parameter to calibrate for stochastic models is the number $N$ of scenarios to include in the optimization phase. Under a scenario-based optimization approach, generating the adequate set of scenarios $\Omega$ could be complex due to the high enumeration issue induced by continuous normal distribution [57]. Assessing their probabilities also entails a tremendous effort. A combination of the Monte Carlo sampling methods [56] and the sample average approximation technique (SAA) [57] helps in finding a good trade-off in terms of the scenario probability estimation and the sufficient number of scenarios to consider in the model. This approach has been applied to network design problems in [54] and to stochastic multi-period location transportation problem in [31]. The SAA consists in generating for each time period $t$, before the optimization procedure, an independent sample of $N$ equiprobable scenarios $\Omega^N_t \subset \Omega_t$ from the initial probability distribution, which removes the need to explicitly compute the scenario demand probabilities $p(\omega)$. The quality of the solution obtained with this approach improves as the scenario sample size $N$ increases. However, one would choose $N$ taking into account the trade-off between the quality of the obtained design and the computational effort needed to solve the problem. Thus, to determine the best value of $N$, solving the problem with $M$ independent samples of demand repeatedly can be more efficient. This leads to a maximum of $M$ different design decisions – i.e. location and capacity allocation. It is worth to note that some samples may provide identical design decisions. The average value of the $M$ expected costs based on the $N$ scenarios gives a statistical lower bound. Then, we evaluate the obtained designs based on the expected daily routing cost. We fix the first-stage decisions according to each of these different designs and solve the resulting problem for $N' = |\Omega^{N'}_t| \gg N$ independent scenarios to get an upper bound on the optimal solution of the problem. Finally, a statistical optimality gap is computed for each obtained design from these lower and upper bounds. For more details, interested reader is referred to [54] and [55]. We notice that an external recourse option is added here, at a high cost,

Table 3: Average statistical optimality gap values for (I1,LT,TC,NIT) instances

| $\text{Gap}_{N,120}$ (in %) | | | | |
|---|---|---|---|---|
| Problem size | Sample size ($N$) | | | |
| | 5 | 10 | 15 | 25 |
| 5-4/8/15-$N$- | 2.11 | 0.85 | 0.39 | -0.14 |
| 5-4/8/20-$N$- | 2.55 | 1.07 | 1.14 | 0.34 |

in order to guarantee the feasibility of all scenarios.

To apply the SAA technique, we solved $M = 10$ demand samples and used sample sizes of $N = 5, 10, 15$ and 25 scenarios for each time period $t$. The best feasible solution of each SAA sample is then stored as a candidate solution for valuation in the reference sample. The size of the reference sample per period $t$ is set to $N' = |\Omega_t^{N'}| = 120$ scenarios. The average gap values for problem sizes 5-4/8/15-$N$- and 5-4/8/20-$N$- under (I1,LT,TC,NIT) instance configuration using the different values of $N$ are summarized in Table 3.

Table 3 shows that the optimality gap improves as the sample size $N$ increases and converges to 0%. Samples of $N = 15$ and 25 scenarios provide satisfactory results, optimality gap is generally less than 1% for both instances. Moreover, we note that the decisions produced with alternative samples ($M = 10$) present a high similarity in terms of the opened DPs and the inbound allocation. However, the solution time increases considerably with the sample size. Accordingly, the sample size of $N = 15$ is retained as the best trade-off to use in the experiments for instances with 50 customers and $N = 25$ is selected for instances with 15 and 20 customers. Recall that when $N$ scenarios are used in the SAA model, $5 \times N$ instances are then sampled from the probability distribution as the planning horizon includes 5 periods.

## 5.3 Results

In this section, we evaluate the performance of the proposed Benders approach and provide an analysis of the design solutions produced by the algorithm. Further, we examine the sensitivity of the WP and DP location decisions to the uncertainty in various problem attributes, and the behavior of the capacity decision in a multi-period and uncertain setting.

In order to evaluate the performance of our approach, we solve the deterministic equivalent formulation (DEF) of the problem using a commercial solver (Cplex). To this end, in the DEF, we reformulate the CVRP-CMD as a three-index vehicle-flow formulation as introduced in [60]. Two instances of size 5-4/8/15-1- and 5-4/8/20-1- under attributes (I1, LT, LC, NIT) are tested. The results show that Cplex is not able to solve these two instances with one scenario to optimality and stops after 13 hours due to lack of memory with an optimality gap of 13% for 5-4/8/15-1- instance and 25% for 5-4/8/20-1- instance.

Then, the nine instances given in Table 1 are solved using the proposed Benders approach. The results are reported in Table 4. The first two columns present the instance attribute and size associated with the sample size $N$. The third column *#Opt* presents the number of optimal solutions found under each scenario sample size $N$. The next three columns *#CombCuts*, *#OptCuts* and *#Iter* provide the average number of generated combinatorial Benders cuts (28)–(36), Benders optimality cuts (24) and the required number of iterations for convergence, respectively. The column *Gap(%)* indicates the average optimality gap. The three next columns under the heading *Parallel computing time* give the average CPU time spent for solving the Benders master problem (MP), the $T \times N$ CVRP-CMD subproblems and the total time needed to obtain an optimal solution of the problem using parallel computing. This average is computed over the instances that could be solved within the time limit ($72\,hours$). For comparison purposes, the last column presents the total running time using sequential computing for the solved problems. It is worth noting that the total time includes the MP time, the CVRP-CMD time and the BPP time.

Table 4 shows that the developed approach is able to solve most instances within a reasonable time with an $\epsilon = 0.05\%$ optimality. It solves all instances of 15 and 20 customers, in less than 30 minutes average time with parallel computing. Note that for instances with 15 customers, solving the BPP takes the most computational time (2 to 7 minutes) compared to the MP+CVRP-CMD time. This is essentially due to the sequential computing of the BPP for each period and each scenario. The sequential computing time demonstrates that the parallel computing reduces the running time drastically, mainly for moderate-size instances with 20 customers, as the sequential solving approach could take from 4 to 10 times longer for such instances, reaching an average running time of 5 hours 25 minutes – which are solved in about 30 minutes on average with parallelization. Also worth noting is that most computing time (about 70%) is spent by the branch-cut-and-price to get an integer solution to the $T \times N$ CVRP-CMD subproblems (see Table 10 in Appendix B for details). This justifies the use of a parallel computing approach to solve the $T \times N$

Table 4: Average results per problem-instance

| Instance | $N$ | #Opt | #CombCuts | #OptCuts | #Iter | Gap(%) | Parallel computing time | | | Sequential computing time |
|---|---|---|---|---|---|---|---|---|---|---|
| | | | | | | | MP | CVRP-CMD | total | |
| 5-4/8/15- | 5 | 24/24 | 2 | 6.3 | 8.5 | 0.00 | 4s | 50s | 2m47s | 3m48s |
| | 10 | 24/24 | 1.9 | 6.3 | 8.1 | 0.01 | 5s | 50s | 4m6s | 6m55s |
| | 15 | 24/24 | 1.9 | 6.3 | 8.2 | 0.00 | 6s | 1m4s | 5m51s | 8m39s |
| | 25 | 24/24 | 2 | 6.7 | 8.7 | 0.00 | 9s | 1m27s | 9m21s | 13m49s |
| 5-4/12/15- | 5 | 15/15 | 1.9 | 6.8 | 8.7 | 0.00 | 8s | 47s | 2m32 | 8m20s |
| | 10 | 15/15 | 2 | 7.4 | 9.4 | 0.00 | 12s | 59s | 4m22s | 11m32s |
| | 15 | 15/15 | 2.1 | 7.3 | 9.3 | 0.00 | 15s | 1m8s | 6m5s | 18m2s |
| | 25 | 15/15 | 2.1 | 7.5 | 9.6 | 0.00 | 25s | 1m28s | 9m44s | 24m7s |
| 5-4/16/15- | 5 | 12/12 | 2.25 | 7.3 | 9.6 | 0.00 | 12s | 2m35s | 4m24s | 11m39s |
| | 10 | 12/12 | 2.3 | 7 | 9.3 | 0.00 | 20s | 1m | 4m34s | 11m29s |
| | 15 | 12/12 | 2.3 | 7.25 | 9.5 | 0.00 | 24s | 1m11s | 6m24s | 17m29s |
| | 25 | 12/12 | 1.9 | 7 | 8.9 | 0.01 | 27s | 1m32s | 9m50s | 38m21s |
| 5-4/8/20- | 5 | 24/24 | 2.1 | 9 | 11.1 | 0.00 | 6s | 1m19s | 3m39s | 36m7s |
| | 10 | 24/24 | 2.1 | 8.7 | 10.7 | 0.00 | 7s | 2m40s | 7m14s | 1h2m |
| | 15 | 24/24 | 1.9 | 8.8 | 10.7 | 0.01 | 10s | 3m23s | 10m15s | 1h46m |
| | 25 | 24/24 | 2.1 | 9 | 11.1 | 0.00 | 16s | 5m48s | 17m14s | 1h59m |
| 5-4/12/20- | 5 | 15/15 | 2.1 | 9.3 | 11.5 | 0.00 | 12s | 2m28s | 4m55s | 39m9s |
| | 10 | 15/15 | 1.9 | 8.5 | 10.5 | 0.01 | 16s | 1m51s | 6m37s | 1h25m |
| | 15 | 15/15 | 2 | 8.7 | 10.7 | 0.00 | 22s | 5m26s | 12m29s | 2h11m |
| | 25 | 15/15 | 1.9 | 7.9 | 9.9 | 0.00 | 30s | 14m21s | 26m3s | 1h34m |
| 5-4/16/20- | 5 | 12/12 | 1.9 | 8.8 | 10.75 | 0.00 | 16s | 1m47s | 4m20s | 29m2s |
| | 10 | 12/12 | 2.2 | 9.7 | 11.8 | 0.01 | 37s | 2m59s | 8m7s | 1h10m |
| | 15 | 12/12 | 2.5 | 9.9 | 12.4 | 0.00 | 1m3s | 11m47s | 18m33s | 2h49m |
| | 25 | 12/12 | 2.25 | 9.67 | 11.91 | 0.01 | 1m34s | 18m9s | 30m56s | 5h25m |
| 5-4/8/50- | 15 | 9/15 | 7.4 | 20.4 | 27.8 | 0.03 | 39m13s | 16h54s | 17h54m | |
| 5-4/12/50- | 15 | 8/15 | 7.1 | 26.5 | 33.6 | 0.03 | 2h50m | 13h3m | 16h14m | |
| 5-4/16/50- | 15 | 9/12 | 4.8 | 19.7 | 24.7 | 0.02 | 35m48s | 7h34m | 8h52m | |

CVRP-CMD subproblems.

Furthermore, when the large-scale instances with 50 customers concerned, proposed algorithm is able to solve optimally 26 out of 42 instances within an average time of 14 hours 20 minutes. The average optimality gap in the remaining 16 instances is generally below 0.5% which underlines the efficacy of the developed Benders approach. These instances are not solvable with the sequential approach within the maximum allocated time, as solving the $T \times N$ CVRP-CMD subproblems is time consuming. Moreover, Table 4 emphasizes the inherent complexity of the stochastic setting where computing time grows as the size of the scenarios sample $N$ increases. Additionally, the Benders master problem (MP) takes only few seconds to be solved in most of the instances with 15 and 20 customers and grows up to two hours in the instances (5-4/12/50-.) using 15 scenarios. The MP resolution is also highly correlated with the number of potential DPs in the considered instance. The increase in computing time here is mainly due to the large number of cuts that are added to the relaxed MP in each iteration.

We next evaluate the performance of the solution approach with respect to the combination of problem attributes: customer dispersion, transportation cost, capacity configuration and demand process, as defined in Section 5.1. Table 5 shows the results obtained for instances with 8 DPs and 15, 20, 50 customers, respectively, in terms of the best upper bound (ub), the best lower bound (lb), the optimality gap (%), and the computation time. For consistency purpose, for each instance, three random instantiation of the input parameters is made as indicated in the second column. For problem instances with 12 DPs and 16, the results are provided in Tables 11 and 12, respectively, in Appendix B.

We observe that instances under large capacity attribute (LC) are easier to solve than the other attributes, and are all solved to optimality. Nevertheless, the tight capacity attribute (TC) makes data set more difficult to solve. Only few instances with 50 customers are solved within the time limit and the other ones present a reduced gap, below 1%. This is consistent with former results on capacitated LRPs and VRPs. Furthermore, the instances with network configuration I2 are solved more efficiently compared to I1-based instances. This is mainly due to the fact that in I2, where customers are more dispersed in the urban area (Figure 3(b)),the routing subproblems are easier to solve. Indeed, two instances out of three with 50 customers are optimally solved under I1, whereas all three instances are solved to optimality under I2. Cost attribute also impacts the complexity of the problem. In fact, for 5-4/8/50-15-(I1,.,TC,NIT), two instances out of three are optimally solved under LT attribute. However, no optimality is obtained under the HT attribute. This is mainly due to the increase of transportation costs under HT, which makes location-routing cost trade-offs more contrasting. A difference in solvability is also observed regarding

Table 5: Detailed results for 5-4/8/15-25-, 5-4/8/20-25- and 5-4/8/50-15-

| | | 5-4/8/15-25- | | | | 5-4/8/20-25- | | | | 5-4/8/50-15- | | | |
|---|---|---|---|---|---|---|---|---|---|---|---|---|---|
| | | ub | lb | Gap(%) | Time | ub | lb | Gap(%) | Time | ub | lb | Gap(%) | Time |
| (I2, LT, TC, NIT) | 1 | 74486.0 | 74486.0 | 0.0 | 10m36s | 82611.2 | 82611.2 | 0.0 | 12m52 | 205012.0 | 204953.0 | 0.03 | 3h49m |
| | 2 | 72344.1 | 72344.1 | 0.0 | 8m55s | 96468.5 | 96468.5 | 0.0 | 13m19s | 188933.0 | 188856.0 | 0.04 | 53h50m |
| | 3 | 84334.7 | 84334.7 | 0.0 | 8m58s | 89290.4 | 89290.4 | 0.0 | 33m53s | 200191.0 | 200116.0 | 0.04 | 18h9m |
| **average** | | 77054.9 | 77054.9 | 0.0 | 9m30s | 89456.7 | 89456.7 | 0.0 | 20m2s | 194562.0 | 194486.0 | 0.04 | 36h |
| (I1, LT, TC, NIT) | 1 | 74387.2 | 74387.2 | 0.0 | 9m44s | 91276.5 | 91276.5 | 0.0 | 14m43s | 203537.8 | 203367.7 | 0.08 | - |
| | 2 | 73465.3 | 73465.3 | 0.0 | 8m48s | 84255.3 | 84255.3 | 0.0 | 13m40s | 187485.0 | 187396.0 | 0.05 | 56h16m |
| | 3 | 82051.9 | 82051.9 | 0.0 | 9m30s | 89212.5 | 89212.5 | 0.0 | 28m4s | 199104.0 | 199045.0 | 0.03 | 6h53m |
| **average** | | 76634.8 | 76634.8 | 0.0 | 9m21 | 88248.1 | 88248.1 | 0.0 | 18m49s | 196708.9 | 196602.9 | 0.05 | 31h34m |
| (I1, HT, TC, NIT) | 1 | 104470.0 | 104470.0 | 0.0 | 10m21s | 128554.0 | 128554.0 | 0.0 | 15m54s | 286317.3 | 286003.7 | 0.11 | - |
| | 2 | 103992.0 | 103992.0 | 0.0 | 9m24s | 123425.0 | 123425.0 | 0.0 | 13m52s | 268163.6 | 267670.7 | 0.18 | - |
| | 3 | 113685.0 | 113685.0 | 0.0 | 9m56s | 126692.0 | 126692.0 | 0.0 | 21m18s | 283578.6 | 282502.6 | 0.38 | - |
| **average** | | 107382.3 | 107382.3 | 0.0 | 9m54s | 126223.7 | 126223.7 | 0.0 | 17m2s | 279353.2 | 278725.7 | 0.22 | - |
| (I1, LT, LC, NIT) | 1 | 84275.7 | 84275.7 | 0.0 | 8m54s | 96880.2 | 96880.2 | 0.0 | 12m41s | 190453.0 | 190453.0 | 0.0 | 35m10s |
| | 2 | 82808.3 | 82808.3 | 0.0 | 8m30s | 100817.0 | 100817.0 | 0.0 | 13m41s | 188179.0 | 188179.0 | 0.0 | 34m5s |
| | 3 | 86280.8 | 86280.8 | 0.0 | 9m34s | 93665.0 | 93665.0 | 0.0 | 20m36s | 196985.0 | 196898.0 | 0.04 | 1h16m |
| **average** | | 84454.9 | 84454.9 | 0.0 | 9m | 97120.7 | 97120.7 | 0.0 | 15m40s | 191872.3 | 191843.3 | 0.01 | 48m25s |
| (I1, LT, TC, NVT) | 1 | 75856.1 | 75856.1 | 0.0 | 9m4s | 107509.0 | 107465.0 | 0.04 | 13m22s | 189925.8 | 189346.1 | 0.31 | - |
| | 2 | 57568.5 | 57568.5 | 0.0 | 8m46s | 96637.7 | 96637.7 | 0.0 | 16m56s | 218641.0 | 218553.0 | 0.04 | 19h43m |
| | 3 | 82664.3 | 82664.3 | 0.0 | 9m13s | 98871.2 | 98871.2 | 0.0 | 13m41s | 208253.5 | 208028.5 | 0.11 | - |
| **average** | | 72029.6 | 72029.6 | 0.0 | 9m1s | 101006.0 | 100991.3 | 0.01 | 14m40s | 205606.8 | 205309.2 | 0.15 | 19h43m |

the demand process attribute. Instances under NVT process are more difficult to solve compared to those under NIT, which is due to the augmented variability of the demand process in the former. As seen in Table 5 for instance, one instance sized 5-4/8/50-15-(I1,LT,TC,.) is optimally solved under NVT process compared to two under NIT.

Table 6: Location decisions and their operating periods for 5-4/./20-25-(.,.,.,.)-3

| | (I1,LT,TC,NIT) | | | (I1,HT,TC,NIT) | | | (I1,LT,TC,NVT) | | | (I1,LT,LC,NIT) | | | Presence (%) |
|---|---|---|---|---|---|---|---|---|---|---|---|---|---|
| $\|\mathcal{L}\|$ | 8 | 12 | 16 | 8 | 12 | 16 | 8 | 12 | 16 | 8 | 12 | 16 | |
| $\underline{l1}$ | 0 | 0 | 0 | 0 | 0 | 0 | 0 | 0 | 0 | 0 | 0 | 0 | 0 |
| $\underline{l2}$ | 0 | 0 | 0 | 0 | 0 | 0 | 0 | 0 | 0 | 0 | 0 | 0 | 0 |
| l3 | 0 | 0 | 0 | 0 | 0 | 0 | 1 | 1 | 0 | 0 | 0 | 0 | 14 |
| l4 | 1 | 0 | 1 | 1 | 0 | 0 | 0 | 0 | 1 | 0 | 0 | 0 | 35 |
| l5 | 0 | 2 | 0 | 0 | 2 | 0 | 0 | 0 | 0 | 1 | 0 | 0 | 29 |
| l6 | 1 | 0 | 0 | 1 | 0 | 0 | 1 | 0 | 0 | 0 | 0 | 0 | 29 |
| l7 | 0 | 0 | 0 | 0 | 0 | 0 | $2^{\star}$ | 1 | 0 | 0 | 1 | 0 | 21 |
| l8 | 0 | 0 | 0 | 0 | 0 | 0 | 0 | 0 | 0 | 0 | 0 | 0 | 0 |
| $\underline{l9}$ | | 0 | 0 | | 0 | 0 | | 0 | 0 | | 0 | 0 | 0 |
| l10 | | 0 | 0 | | 0 | 0 | | 0 | 0 | | 0 | 0 | 0 |
| l11 | | 0 | 0 | | 0 | 0 | | 0 | 0 | | 0 | 0 | 7 |
| l12 | | 1 | 0 | | 1 | 0 | | 0 | 0 | | 0 | 0 | 14 |
| $\underline{l13}$ | | | 0 | | | 0 | | | 0 | | | 0 | 0 |
| l14 | | | 0 | | | 1 | | | 0 | | | 1 | 14 |
| l15 | | | 1 | | | 1 | | | 1 | | | 0 | 21 |
| l16 | | | 0 | | | 0 | | | 0 | | | 0 | 0 |
| Closed at t= | | | | | | | 5 | | | | | | |

We next closely look at the design decisions produced by our model. The results are presented in Tables 6 and 7 for the different problem sizes with 20 and 50 customers, respectively. The results for instances with 15 customers are given in Table 13 in Appendix B. These tables present the DP opening decisions and their operating periods: value 0 refers to DPs kept closed and a value in the range $[1, 5]$ corresponds to the DP opening period $t$. A star ($^{\star}$) or a diamond ($^{\diamond}$) symbol indicates that the DP has been closed and the closing period is given at the last row. No symbol means that the DP has kept operating until the end of the planning horizon. The first row corresponds to the combination of attributes and the second row provides the size of potential DPs. The first column corresponds to the list of potential DPs. The underlined DPs are those located in the central urban area *Area3* of the network. Tables 6 and 7 reveal that the opened DP number increases as the customer size grows, since it impacts the total demand level of the network. Under tight capacity attribute (TC), two to three DPs are opened for instances with 20 customers. This number reaches to six for instances with 50 customers. Nevertheless, under large capacity (LC), the number of opened DPs is smaller compared to the ones under TC as DPs can, in the former case, accommodate more inbound flows from WPs. Regarding WPs, the opened number is quite stable in the instances: three WPs at most are opened

Table 7: Location decisions and their operating periods for 5-4/./50-15-(.,.,.,.)-3

| | (I1,LT,TC,NIT) | | | (I1,HT,TC,NIT) | | | (I1,LT,TC,NVT) | | | (I1,LT,LC,NIT) | | | Presence (%) |
|---|---|---|---|---|---|---|---|---|---|---|---|---|---|
| $\|\mathcal{L}\|$ | 8 | 12 | 16 | 8 | 12 | 16 | 8 | 12 | 16 | 8 | 12 | 16 | |
| l1 | 0 | 0 | 0 | 0 | 0 | 0 | 0 | 0 | 0 | 0 | 0 | 0 | 0 |
| l2 | 0 | 0 | 0 | 0 | 0 | 0 | 1 | 0 | 0 | 0 | 0 | 0 | 7 |
| l3 | 4 | 0 | 0 | 2 | 1 | 0 | 0 | 1 | 0 | 0 | 0 | 0 | 42 |
| l4 | 1 | 1 | 1 | 1 | 0 | 1 | 1 | $2^{\star}$ | 1 | 0 | 1 | 1 | 85 |
| l5 | 1 | 1 | 0 | 1 | 2 | 0 | $1^{\star}$ | 1 | 0 | 1 | 0 | 0 | 64 |
| l6 | 2 | 0 | 0 | 4 | 0 | 0 | $1^{\diamond}$ | 0 | 0 | 0 | 0 | 0 | 28 |
| l7 | 1 | 1 | 2 | 1 | 1 | 1 | 3 | 1 | 2 | 0 | 1 | 1 | 92 |
| l8 | 0 | 0 | 0 | 0 | 0 | 0 | 0 | 0 | 0 | 1 | 0 | 0 | 14 |
| l9 | | 0 | 0 | | 0 | 0 | | 0 | 0 | | 0 | 0 | 0 |
| l10 | | 4 | 0 | | 0 | 0 | | 0 | 0 | | 0 | 0 | 7 |
| l11 | | 0 | 1 | | 4 | 1 | | 0 | 3 | | 0 | 0 | 28 |
| l12 | | 1 | 0 | | 1 | 0 | | 1 | 1 | | 0 | 0 | 35 |
| l13 | | | 0 | | | 0 | | | 0 | | | 0 | 0 |
| l14 | | | 0 | | | 0 | | | 0 | | | 0 | 0 |
| l15 | | | 4 | | | 4 | | | $1^{\star}$ | | | 0 | 21 |
| l16 | | | 1 | | | 1 | | | 0 | | | 0 | 14 |
| Closed at t= | | | | | | | $^{\star}5,^{\diamond}4$ | $^{\star}4$ | $^{\star}5$ | | | | |

for instances with 50 customers.

Additionally, the location of both WPs and DPs and the throughput capacity levels are correlated with the demand process, the customers dispersion, and costs. The results highlight the sensitivity of the strategic location decisions as in several cases, the design structure varies between high and low transportation cost. For instance, we observe in Table 6 with 5-4/8/20-25-(I1,LT,TC,NIT) that the network opened DPs 4 and 6, whereas with 5-4/8/20-25-(I1,HT,TC,NIT), DPs 3 and 7 are opened. We noticed that only in few instances the centralized DPs – i.e., the ones positioned in *Area3* which are underlined in the tables – were opened, which is due to their higher fixed costs. In addition, the customer dispersion – i.e., I1 vs I2 – impacts the DP location decisions, mainly under (.,LT,TC,NIT) attributes, as illustrated in Table 8. For example, for the instance size 5-4/12/50-15-, DPs 4, 5, 7, 8 and 12 are opened under I2 attribute instead of 4, 5, 7, 10 and 12 under I1. Even though the DP 12 is opened under both attributes settings, the timing is not the same – i.e., opening period $t = 1$ for I1 and $t = 4$ for I2.

Table 8: Location decisions and their operating periods for the customer dispersion attribute (I1 vs I2)

| | 5-4/./20-25- | | | | 5-4/./50-15- | | | |
|---|---|---|---|---|---|---|---|---|
| | (I1,LT,TC,NIT) | | (I2,LT,TC,NIT) | | (I1,LT,TC,NIT) | | (I2,LT,TC,NIT) | |
| $\|\mathcal{L}\|$ | 8 | 12 | 8 | 12 | 8 | 12 | 8 | 12 |
| l1 | 0 | 0 | 0 | 0 | 0 | 0 | 0 | 0 |
| l2 | 0 | 0 | 0 | 0 | 0 | 0 | 0 | 0 |
| l3 | 0 | 0 | 0 | 0 | 4 | 0 | 3 | 0 |
| l4 | 1 | 0 | 1 | 0 | 1 | 1 | 1 | 1 |
| l5 | 0 | 2 | 0 | 1 | 1 | 1 | 1 | 1 |
| l6 | 1 | 0 | 1 | 0 | 2 | 0 | 1 | 0 |
| l7 | 0 | 0 | 0 | 0 | 1 | 1 | 1 | 1 |
| l8 | 0 | 0 | 0 | 0 | 0 | 0 | 0 | 1 |
| l9 | | 0 | | 0 | | 0 | | 0 |
| l10 | | 0 | | 0 | | 4 | | 0 |
| l11 | | 0 | | 1 | | 0 | | 0 |
| l12 | | 1 | | 0 | | 1 | | 4 |
| Closed at t= | | | | | | | | |

Moreover, the presence of additional potential DPs has an impact on the location decisions. In general, we observe a very low similarity in the location of DPs between instances with 8, 12 and 16 DPs, respectively. Looking closely at the instance with 20 customers in Table 6, no identical DP location is observed under (I1,HT,TC,NIT) configuration. However, under (I1,LT,TC,NIT), the instances 5-4/8/20-25- and 5-4/16/20-25- have 4 DPs in common. Additionally, the change in truck capacities impacts the location decisions as illustrated in instances 5-4/./50-15 under (I1,LT,LC,NIT).

Furthermore, a key finding is the sensitivity to the demand uncertainty in terms of location decisions and capacity decisions. The results justifies the multi-period design setting. In fact, we notice in almost all cases that the opening decisions follow the trend function and are planned over the different design periods. For instance, under the (I1,LT,TC,NIT) configuration, the problem size 5-4/12/20-25- fixes DP 12 from the first design period, and further at period $t = 2$ it opens DP 5. The same instance under the NVT demand process fixes all the opening locations from the first design period. The instance 5-4/8/20-25-(I1,LT,TC,NVT) also attests to the necessity of the multi-period

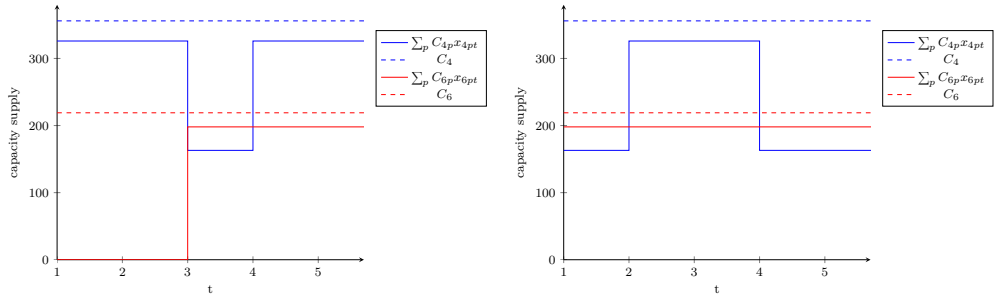


(a) NIT process (b) NVT process

Figure 4: Capacity-allocation decisions from multi-period modeling approach versus the a priori capacity $C_l$ for 5-4/8/15-25-(I1,LT,TC,.)

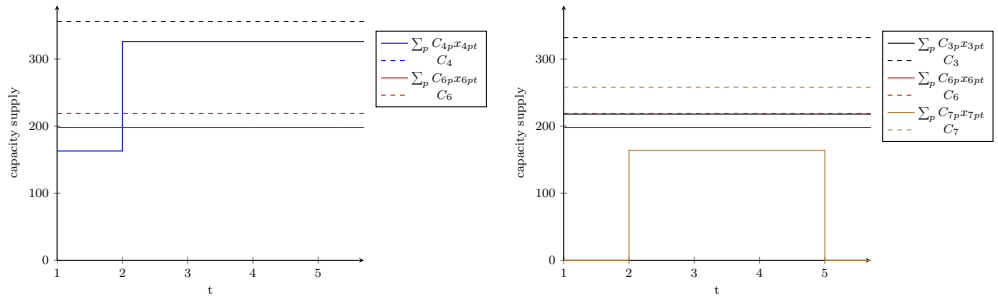


(a) NIT process (b) NVT process

Figure 5: Capacity-allocation decisions from multi-period modeling approach versus the apriori capacity $C_l$ for 5-4/8/20-25-(I1,LT,TC,.)

design flexibility that we propose in this work. We see that DP 7 is opened at $t = 2$ to meet the increasing trend of the demand at periods one to three. This latter is then closed at $t = 5$ as the demand decreases at periods four and five. In several cases, the tables do not show the multi-period opening/closing of location decisions. Instead, the capacity level is adjusted to meet the demand variability which we report in Figures 4 and 5. In addition, we note a high variability in the location of opened DPs when comparing solutions from the two demand processes. To emphasize this result, one can closely observe the instance 5-4/12/20-25-(I1,LT,TC,.) where there is no identical DP for NIT vs NVT. As for 5-4/16/15-25-(I1,LT,TC,.), we obtain 100% identical DPs for NIT vs NVT, but they differ in opening and closing periods (see Table 13). Therefore, the obtained results confirm that the stochastic multi-period demand process is adequately captured by the two-stage stochastic formulation we present in this work.

As a complement to the above analysis, we also investigate the evolution of the capacity decisions in the multi-period and uncertain setting, since in the two-echelon structure, the demand is covered with respect to the inbound allocation to DPs from WPs, and not with a predefined DP capacity. In Figures 4 and 5, we examine in depth the capacity decisions modeled in the 2E-SM-CLRP and contrast it to the evolution of each demand process along the planning horizon. These figures provide the results of instances 5-4/8/15-25-(I1,LT,TC,.) and 5-4/8/20-25-(I1,LT,TC,.) for both the NIT and NVT demand processes which produces a design solution with two or three DPs. Each solid line corresponds to the capacity available at each opened DP in period $t$ – i.e., $\sum_p C_{lp}x_{lpt}$ – and each dashed line its related predetermined capacity $C_l$ where each color represent a separate opened DP. We use the same color if the same DP is opened under both settings. Figure 4 and 5 clearly illustrate the impact of the multi-period modeling approach where the capacity decisions for each opened DP are clearly adapted periodically. Even if the two demand processes of the instance 5-4/8/15-25-(I1,LT,TC,.) produce the same DP location decisions, the capacity decisions behave differently under each demand process to follow the time-varying demand process. This means that the two-stage model for the 2E-SM-CLRP mimics the dynamic capacity model with the inclusion of multi-period capacity decisions.

Table 9: Comparison between static and multi-period modeling approach

| | | | Static modeling approach | | | Cost loss (%) |
|---|---|---|---|---|---|---|
| | | | ub | lb | Gap(%) | |
| 5-4/8/20-25- | (I1,LT,TC,NIT) | 1 | 91585.8 | 91585.8 | 0 | 0.34 |
| | | 2 | 84255.3 | 84255.3 | 0 | 0.0 |
| | | 3 | 90082.1 | 90082.1 | 0 | 0.97 |
| | (I1,HT,TC,NIT) | 1 | 129205 | 129205 | 0 | 0.51 |
| | | 2 | 123425 | 123425 | 0 | 0.0 |
| | | 3 | 128426 | 128383 | 0.03 | 1.37 |
| | (I1,LT,TC,NVT) | 1 | 110947 | 110947 | 0 | 3.2 |
| | | 2 | 98895.8 | 98895.8 | 0 | 2.34 |
| | | 3 | 99970.8 | 99970.8 | 0 | 1.11 |
| 5-4/8/50-15- | (I1,LL,TC,NIT) | 1 | 208249.7 | 208181.9 | 0.03 | 2.31 |
| | | 2 | 192102.2 | 192066.5 | 0.02 | 2.46 |
| | | 3 | 206563.9 | 205694.3 | 0.42 | 3.75 |
| | (I1,HT,TC,NIT) | 1 | 292578.7 | 292541.7 | 0.01 | 2.19 |
| | | 2 | 276247.5 | 276170.9 | 0.03 | 3.01 |
| | | 3 | 292412.5 | 292281.1 | 0.04 | 3.12 |
| | (I1,LT,TC,NVT) | 1 | 194168.8 | 194130.8 | 0.02 | 2.23 |
| | | 2 | 231215.2 | 231184.8 | 0.01 | 5.75 |
| | | 3 | 216878.5 | 216770.3 | 0.05 | 4.14 |
| 5-4/12/20-25- | (I1,LT,TC,NIT) | 1 | 79842.3 | 79842.3 | 0 | 0.00 |
| | | 2 | 88448.6 | 88425 | 0.03 | 0.04 |
| | | 3 | 84441.5 | 84441.5 | 0 | 1.96 |
| | (I1,HT,TC,NIT) | 1 | 117079 | 117079 | 0 | 0.00 |
| | | 2 | 126107 | 126078 | 0.02 | 0.00 |
| | | 3 | 121762 | 121762 | 0 | 1.56 |
| | (I1,LT,TC,NVT) | 1 | 98547.9 | 98547.9 | 0 | 1.76 |
| | | 2 | 94633.7 | 94633.7 | 0 | 2.33 |
| | | 3 | 92953.5 | 92953.5 | 0 | 0.00 |
| 5-4/12/50-15- | (I1,LT,TC,NIT) | 1 | 192350.3 | 192350.3 | 0 | 1.87 |
| | | 2 | 186311.6 | 186311.6 | 0 | 2.35 |
| | | 3 | 194780.5 | 194651.3 | 0.07 | 3.12 |
| | (I1,HT,TC,NIT) | 1 | 281270.5 | 281136 | 0.04 | 2.24 |
| | | 2 | 270558 | 270492.9 | 0.02 | 2.85 |
| | | 3 | 281297.2 | 281042.4 | 0.1 | 3.27 |
| | (I1,LT,TC,NVT) | 1 | 186052.5 | 185785.7 | 0.14 | 2.40 |
| | | 2 | 224365.8 | 224352.7 | 0.005 | 4.58 |
| | | 3 | 203203.1 | 203143.9 | 0.03 | 4.55 |

## 5.4 Multi-period design setting vs static setting

In this section, we further explore the multi-period design setting and compare it to the static modeling approach, in which all design decisions should be fixed from the first design period and no further design changes is possible over the planning horizon. Table 9 provides the best upper and lower bounds from the static design modeling approach, the optimality gap(%) as well as an evaluation of the cost loss with respect to the multi-period approach – i.e., $\frac{\left(ub^{static} - ub^{multi-period}\right)}{ub^{multi-period}} \times 100$.

In Table 9, we observe that in almost all cases the static design setting provides higher expected cost. The cost loss increases with the problem size and it reaches more than 5%. The largest losses are observed under the NVT process as it presents more variability. This is in accordance with the static setting as the model anticipates the DP openings and the required capacity level at design period one and does not allow further changes at the subsequent periods resulting in an over-estimation of the capacity allocated. In other instances as in 5-4/12/20-25-(I1,LT,TC,NIT)-1, we observe that both models converge to the same optimal value. This is explained by the fact that particular instance fixes its design decisions from the first period under the multi-period design setting. This behavior is generally detected with small instances of 15 or 20 customers, and are mostly under NIT process. In addition, the static approach can solve optimally instances that cannot be solved with the multi-period setting, as it is the case of 5-4/8/50-15- under (I1,HT,TC,NIT) attributes. It is worth noting that a high variability of the solutions in terms of location and capacity is observed between both modeling approaches. For further illustration, see the results reported in Table 14 in Appendix B.

We complete our analysis by reporting the obtained capacity decisions for instance 5-4/8/20-25-(I1,LT,TC,.) under both demand processes using the static setting in Figure 6. Each opened DP is represented with a color in the figure. For comparison purpose, we also mention in Figure 6 the capacity obtained using the multi-period approach. From Figure 6(a), under the NIT process, we notice that both static and multi-period modeling settings converge to the same location openings, but therein the static setting fixes all its capacity at the first period for DP 4 contrary to the multi-period approach. Under the NVT process, both approaches have only DP 3 in common fixing the same

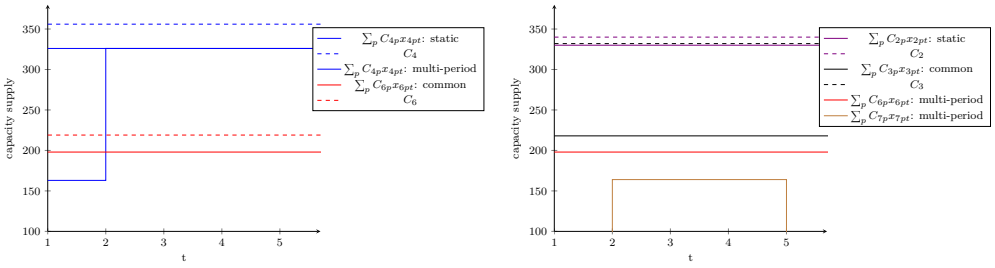


(a) NIT process (b) NVT process

Figure 6: Capacity-allocation decisions from static modeling approach versus the a priori capacity $C_l$ for 5-4/8/20-25-(I1,LT,TC,.)

level of capacity from the beginning of the planning horizon. As mentioned, the static approach over-estimates its capacity level to hedge against the variability of the demand. Looking closely at the aforementioned example, the system allocates in total about 2620 units of capacity with the static setting versus 2457 for the multi-period case under the NIT process (resp, 2740 vs 2572 under NVT). Therefore, one can conclude about the effectiveness of the multi-period modeling approach, as it offers the flexibility to adapt its hedging capabilities over time.

# 6. Conclusion

In this paper, we have addressed the two-echelon stochastic multi-period capacitated location-routing problem (2E-SM-CLRP). The problem is characterized as a hierarchical decision process involving a design level in which network location and capacity allocation decision are taken, and an operational level dealing with transportation decisions of the second echelon. A stochastic multi-period characterization of the planning horizon is considered, shaping the evolution of the uncertain customer demand and costs. This temporal hierarchy is formulated as a two-stage stochastic integer program with recourse. To solve the 2E-SM-CLRP, we have presented an exact Benders decomposition algorithm. In the first-stage, location (WPs and DPs) and capacity assignment decisions are taken by solving the Benders master problem. When these first-stage decisions are fixed, the resulting subproblem is a capacitated vehicle-routing problem with capacitated multi-depot (CVRP-CMD) which is further decomposed by period and scenario. Each CVRP-CMD is then solved using the state-of-the-art branch-cut-and-price algorithm. Combinatorial Benders cuts are also proposed to cut off the current solution to converge to the optimal solution of the 2E-SM-CLRP. To the best of our knowledge, this is the first exact method that has been proposed for this class of problems. The proposed method is able to solve optimally realistic instances containing up to 50 customers and 25 demand scenarios under a 5-year planning horizon, and provides good lower bounds for the instances that it cannot solve to optimality within the time limit. Extensive computational experiments provide relevant managerial insights regarding the impact of uncertainty on the 2E-SM-CLRP, in addition to the effectiveness of multi-period modeling setting.

Although the Benders decomposition provides good solutions, its performance is limited for large-scale instances. It might be worthwhile improving the proposed algorithm to reduce the running time. In some instances with 50 customers, the CVRP-CMD cannot be solved in an hour, whereas all multi-depot CVRP instances in the literature are solved within the time limit. This points out the complexity of the CVRP-CMD involved in the 2E-SM-CLRP, with respect to the uncapacitated variant. Thus, it would be interesting to develop new valid inequalities adapted to the CVRP-CMD to strengthen the model. Another interesting research direction would be to develop an efficient heuristic solution method adapted to the 2E-SM-CLRP to solve larger problem instances. Future research could focus on more realistic features such as synchronization constraints at intermediate distribution platforms, and constraints limiting route length. Moreover, since routing decisions are often used to anticipate the decision of the operational level, another research perspective of this work would be to examine the route approximation formulæ instead of explicitly computing the vehicle routes. This may speed up the decision process significantly. Last but not least, it would be interesting to add risk measures to the objective function, such as mean semi-deviation and conditional-value-at-risk.

# References


[1] S. Ahmed, A. Shapiro, and E. Shapiro. The sample average approximation method for stochastic programs with integer recourse. *E-print available at* `http://www.optimization-online.org`, 2002.

[2] M. Albareda-Sambola, E. Fernández, and G. Laporte. Heuristic and lower bound for a stochastic location-routing problem. *European Journal of Operational Research*, 179(3):940–955, 2007.

[3] M. Albareda-Sambola, E. Fernández, and S. Nickel. Multiperiod location-routing with decoupled time scales. *European Journal of Operational Research*, 217(2):248–258, 2012.

[4] R. Baldacci, N. Christofides, and A. Mingozzi. An exact algorithm for the vehicle routing problem based on the set partitioning formulation with additional cuts. *Mathematical Programming*, 115(2):351–385, 2008.

[5] R. Baldacci, A. Mingozzi, and R. W. Calvo. An exact method for the capacitated location-routing problem. *Operations Research*, 59(5):1284–1296, 2011.

[6] R. Baldacci, A. Mingozzi, and R. Roberti. New route relaxation and pricing strategies for the vehicle routing problem. *Operations Research*, 59(5):1269–1283, 2011.

[7] R. Baldacci, A. Mingozzi, R. Roberti, and R. W. Calvo. An exact algorithm for the two-echelon capacitated vehicle routing problem. *Operations Research*, 61(2):298–314, 2013.

[8] J. M. Belenguer, E. Benavent, C. Prins, C. Prodhon, and R. W. Calvo. A branch-and-cut method for the capacitated location-routing problem. *Computers & Operations Research*, 38(6):931–941, 2011.

[9] I. Ben Mohamed, W. Klibi, and F. Vanderbeck. Designing a two-echelon distribution network under demand uncertainty. Technical Report, 2018.

[10] J. F. Benders. Partitioning procedures for solving mixed-variables programming problems. *Numerische mathematik*, 4(1):238–252, 1962.

[11] J. R. Birge and F. Louveaux. *Introduction to stochastic programming*. Springer Science & Business Media, 2011.

[12] U. Breunig, V. Schmid, R. F Hartl F, and T. Vidal. A large neighbourhood based heuristic for two-echelon routing problems. *Computers & Operations Research*, 76:208–225, 2016.

[13] C. C. Carøe and J. Tind. L-shaped decomposition of two-stage stochastic programs with integer recourse. *Mathematical Programming*, 83(1-3):451–464, 1998.

[14] C. Contardo, J-F. Cordeau, and B. Gendron. A computational comparison of flow formulations for the capacitated location-routing problem. *Discrete Optimization*, 10(4):263–295, 2013.

[15] C. Contardo, J-F. Cordeau, and B. Gendron. An exact algorithm based on cut-and-column generation for the capacitated location-routing problem. *INFORMS Journal on Computing*, 26(1):88–102, 2013.

[16] C. Contardo, J-F. Cordeau, and B. Gendron. A grasp+ ilp-based metaheuristic for the capacitated location-routing problem. *Journal of Heuristics*, 20(1):1–38, 2014.

[17] C. Contardo, V. C Hemmelmayr, and T. G. Crainic. Lower and upper bounds for the two-echelon capacitated location-routing problem. *Computers & Operations Research*, 39(12):3185–3199, 2012.

[18] T. G. Crainic, S. Mancini, G. Perboli, and R. Tadei. Multi-start heuristics for the two-echelon vehicle routing problem. In *European Conference on Evolutionary Computation in Combinatorial Optimization (EvoCOP)*, volume 6622, pages 179–190, 2011.

[19] T. G. Crainic, N. Ricciardi, and G. Storchi. Advanced freight transportation systems for congested urban areas. *Transportation Research Part C: Emerging Technologies*, 12(2):119–137, 2004.

[20] R. Cuda, G. Guastaroba, and M. G. Speranza. A survey on two-echelon routing problems. *Computers & Operations Research*, 55:185–199, 2015.

[21] G. B. Dantzig and J. H. Ramser. The truck dispatching problem. *Management science*, 6(1):80–91, 1959.

[22] M. S. Daskin. *Network and Discrete Location: Models, Algorithms and Applications.* Wiley-Interscience Publication, New York, 1995.

[23] M. Drexl and M. Schneider. A survey of variants and extensions of the location-routing problem. *European Journal of Operational Research*, 241(2):283–308, 2015.

[24] F. Gao and X. Su. Omnichannel retail operations with buy-online-and-pick-up-in-store. *Management Science*, 63(8):2478–2492, 2016.

[25] J. Gonzalez-Feliu. *Models and methods for the city logistics: The two-echelon capacitated vehicle routing problem.* PhD thesis, Politecnico di Torino, 2008.

[26] S.L. Hakimi. Optimum locations of switching centers and the absolute centers and medians of a graph. *Operations Research*, 12(3):450–459, 1964.

[27] V. C Hemmelmayr. Sequential and parallel large neighborhood search algorithms for the periodic location routing problem. *European Journal of Operational Research*, 243(1):52–60, 2015.

[28] V. C Hemmelmayr, J-F. Cordeau, and T. G. Crainic. An adaptive large neighborhood search heuristic for two-echelon vehicle routing problems arising in city logistics. *Computers & Operations Research*, 39(12):3215–3228, 2012.

[29] S. Irnich and G. Desaulniers. Shortest path problems with resource constraints. In *Column generation*, pages 33–65. Springer, 2005.

[30] M. Jepsen, B. Petersen, S. Spoorendonk, and D. Pisinger. Subset-row inequalities applied to the vehicle-routing problem with time windows. *Operations Research*, 56(2):497–511, 2008.

[31] W. Klibi, F. Lasalle, A. Martel, and S. Ichoua. The stochastic multiperiod location transportation problem. *Transportation Science*, 44(2):221–237, 2010.

[32] W. Klibi, A. Martel, and A. Guitouni. The impact of operations anticipations on the quality of stochastic location-allocation models. *Omega*, 62:19–33, 2016.

[33] G. Laporte. Location-routing problems. In B. L. Golden and A. A. Assad, editors, *Vehicle Routing: Methods and Studies*, pages 163–198. North-Holland, Amsterdam, 1988.

[34] G. Laporte and PJ. Dejax. Dynamic location-routing problems. *Journal of the Operational Research Society*, 40(5):471–482, 1989.

[35] G. Laporte, F. Louveaux, and H. Mercure. Models and exact solutions for a class of stochastic location-routing problems. *European Journal of Operational Research*, 39(1):71–78, 1989.

[36] G. Laporte and F. V. Louveaux. The integer l-shaped method for stochastic integer programs with complete recourse. *Operations Research Letters*, 13(3):133–142, 1993.

[37] G. Laporte and Y. Nobert. A branch and bound algorithm for the capacitated vehicle routing problem. *Operations Research Spektrum*, 5(2):77–85, 1983.

[38] S. Martello and P. Toth. Lower bounds and reduction procedures for the bin packing problem. *Discrete Applied Mathematics*, 28(1):59–70, 1990.

[39] G. Nagy and S. Salhi. Location-routing: Issues, models and methods. *European Journal of Operational Research*, 177(2):649–672, 2007.

[40] V. P. Nguyen, C. Prins, and C. Prodhon. Solving the two-echelon location routing problem by a grasp reinforced by a learning process and path relinking. *European Journal of Operational Research*, 216(1):113–126, 2012a.

[41] V. P. Nguyen, C. Prins, and C. Prodhon. A multi-start iterated local search with tabu list and path relinking for the two-echelon location-routing problem. *Engineering Applications of Artificial Intelligence*, 25(1):56–71, 2012b.

[42] OpenMP Architecture Review Board. The OpenMP API specification for parallel programming. `https://www.openmp.org/`, 2000.

[43] D. Pecin, A. Pessoa, M. Poggi, and E. Uchoa. Improved branch-cut-and-price for capacitated vehicle routing. *Mathematical Programming Computation*, 9(1):61–100, 2017.

[44] G. Perboli and R. Tadei. New families of valid inequalities for the two-echelon vehicle routing problem. *Electronic notes in discrete mathematics*, 36:639–646, 2010.

[45] G. Perboli, R. Tadei, and D. Vigo. The two-echelon capacitated vehicle routing problem: models and math-based heuristics. *Transportation Science*, 45:364–380, 2011.

[46] A. Pessoa, R. Sadykov, E. Uchoa, and F. Vanderbeck. Automation and combination of linear-programming based stabilization techniques in column generation. *INFORMS Journal on Computing*, 30(2):339–360, 2018.

[47] S. Pirkwieser and G. R Raidl. Variable neighborhood search coupled with ilp-based very large neighborhood searches for the (periodic) location-routing problem. In *International Workshop on Hybrid Metaheuristics*, pages 174–189. Springer, 2010.

[48] M. Poggi and E. Uchoa. New exact algorithms for the capacitated vehicle routing problem. In *Vehicle Routing: Problems, Methods, and Applications*, pages 59–86. SIAM, 2 edition, 2014.

[49] C. Prins, C. Prodhon, and R. W. Calvo. Solving the capacitated location-routing problem by a grasp complemented by a learning process and a path relinking. *Quarterly Journal of Operations Research (4OR)*, 4(3):221–238, 2006.

[50] C. Prodhon and C. Prins. A survey of recent research on location-routing problems. *European Journal of Operational Research*, 238(1):1–17, 2014.

[51] L. D. L. Pugliese and F. Guerriero. A survey of resource constrained shortest path problems: Exact solution approaches. *Networks*, 62(3):183–200, 2013.

[52] R. Sadykov, E. Uchoa, and A. Pessoa. A bucket graph based labeling algorithm with application to vehicle routing. Research Report Cadernos do LOGIS 2017/7, Universidade Federal Fluminense, 2017.

[53] S. Salhi and G. K Rand. The effect of ignoring routes when locating depots. *European Journal of Operational Research*, 39(2):150–156, 1989.

[54] T. Santoso, S. Ahmed, M. Goetschalckx, and A. Shapiro. A stochastic programming approach for supply chain network design under uncertainty. *European Journal of Operational Research*, 167(1):96–115, 2005.

[55] P. Schütz, A. Tomasgard, and S. Ahmed. Supply chain design under uncertainty using sample average approximation and dual decomposition. *European Journal of Operational Research*, 199(2):409–419, 2009.

[56] A. Shapiro. Monte carlo sampling methods. *Handbooks in Operations Research and Management Science*, 10:353–425, 2003.

[57] A. Shapiro, D. Dentcheva, and A. Ruszczynski. Lectures on stochastic programming: modeling and theory. *The Society for Industrial and Applied Mathematics and the Mathematical Programming Society, Philadelphia, USA*, 2009.

[58] Z. Shen. Integrated supply chain design models: a survey and future research directions. *Journal of Industrial and Management Optimization*, 3(1):1, 2007.

[59] Z-J. M. Shen and L. Qi. Incorporating inventory and routing costs in strategic location models. *European journal of operational research*, 179(2):372–389, 2007.

[60] C. Sterle. *Location-Routing models and methods for Freight Distribution and Infomobility in City Logistics*. PhD thesis, Università degli Studi di Napoli "Federico II", 2010.

[61] P. Toth and D. Vigo. *Vehicle Routing: Problems, Methods, and Applications*. SIAM, 2 edition, 2014.

[62] R. M. Van Slyke and R. Wets. L-shaped linear programs with applications to optimal control and stochastic programming. *SIAM Journal on Applied Mathematics*, 17(4):638–663, 1969.

[63] F. Vanderbeck, R. Sadykov, and I. Tahiri. Bapcod–a generic branch-and-price code. `https://realopt.bordeaux.inria.fr/?pageid=2`, 2018.

[64] K. Wang, S. Lan, and Y. Zhao. A genetic-algorithm-based approach to the two-echelon capacitated vehicle routing problem with stochastic demands in logistics service. *Journal of the Operational Research Society*, 68(11):1409–1421, 2017.

[65] K. Wang, Y. Shao, and W. Zhou. Matheuristic for a two-echelon capacitated vehicle routing problem with environmental considerations in city logistics service. *Transportation Research Part D: Transport and Environment*, 57:262–276, 2017.

[66] D. Weinswig. Sam's club is closing one-tenth of its stores and converting 12 to e-commerce hubs: Proof that store closures have become respectable? `https://www.linkedin.com/pulse/sams-club-closing-one-tenth-its-stores-converting-12-hubs-weinswig/`, 2018. Accessed: 2018-03-05.

[67] M. Winkenbach, P. R. Kleindorfer, and S. Spinler. Enabling urban logistics services at la poste through multi-echelon location-routing. *Transportation Science*, 50(2):520–540, 2015.

# A. Bin packing problem

In this section, we give the description of the bin packing problem formulated for each period and each scenario, denoted as ($\text{BPP}_{t\omega}$), and present its mathematical formulation. Then, we briefly describe the column generation algorithm used to solve the linear relaxation of the ($\text{BPP}_{t\omega}$).

Consider a large set of bins (i.e. vehicles) with capacity $q$ and a set of $|\mathcal{J}|$ items (i.e. customers) with weights $d_{j\omega t}$ to pack into bins. The objective is to find the minimum number of bins required to pack the set of items so that the capacity of the bins is not exceeded. Let $\mathcal{B}$ be the family of all the subsets of items which fit into one bin, i.e., the solutions to a subproblem. We define the parameter $x_j^B$ that takes 1 if item $j \in \mathcal{J}$ is in set $B \in \mathcal{B}$. Let $\lambda^B$ be the binary variable taking value 1 if the corresponding subset of items $B$ is selected to fill one bin. The set covering reformulation is:

$$\min \sum_{B \in \mathcal{B}} \lambda^B \tag{37}$$

$$\text{S. t.} \quad \sum_{B \in \mathcal{B}} x_j^B \lambda^B \geqslant 1 \qquad j = 1, ..., \mathcal{J} \tag{38}$$

$$\lambda_k \in \{0, 1\} \tag{39}$$

The linear relaxation of (37)-(39) is solved by column generation to provide a lower bound $\Gamma$. This lower bound is obtained by iteratively solving:

- the restricted master problem (RMP) which is the linear relaxation of (37)-(39) with a restricted number of variables;
- and the pricing problem which determines whether there exists a variable $\lambda^B$ to be added to (RMP) in order to improve its current solution; this refers to solve a knapsack problem to get the set $B \in \mathcal{B}$, satisfying capacity constraints, and yielding to the minimum reduced cost column for (RMP).

Let $\pi_j$ be the dual variable associated to constraints (38), the pricing problem for the ($\text{BPP}_{t\omega}$) is written as:

$$\max_{j=1..\mathcal{J}} \pi_j z_j \tag{40}$$

$$\text{S. t.} \quad \sum_{j=1..\mathcal{J}} d_{j\omega t} z_j \leqslant q \tag{41}$$

$$z_j \in \{0, 1\} \qquad j \in \mathcal{J} \tag{42}$$

A column generated by solving the knapsack problem (40)-(42) will terminate column generation procedure in case its reduced cost $1 - \sum_j \pi_j z_j$ turns negative.

We apply the MIP solver *CPLEX* to the pricing formulation (40)-(42). Then, the linear relaxation of (37)-(39) is terminated by LP solver *CPLEX*. This leads to the lower bound $\Gamma$.

# B. Results

Table 10 provides detailed results of the sequential optimization approach.

Table 10: Average results under attributes (.,.,.,.) with sequential approach

| Instance | $N$ | #Opt | #CombCuts | #OptCuts | #Iter | Gap(%) | Sequential computing time | | |
|---|---|---|---|---|---|---|---|---|---|
| | | | | | | | MP | CVRP-CMD | total |
| 5-4/8/15- | 5 | 24/24 | 2 | 6.4 | 8.4 | 0.0 | 30s | 2m | 3m48s |
| | 10 | 24/24 | 1.8 | 6.3 | 8.1 | 0.0 | 40s | 3m33s | 6m55s |
| | 15 | 24/24 | 2 | 6.2 | 8.2 | 0.0 | 1m | 3m40s | 8m39s |
| | 25 | 24/24 | 2 | 6.7 | 8.7 | 0.0 | 1m52s | 5m29s | 13m49s |
| 5-4/12/15- | 5 | 15/15 | 2 | 6.8 | 8.8 | 0.0 | 2m47s | 4m6s | 8m20s |
| | 10 | 15/15 | 1.8 | 7.4 | 9.2 | 0.0 | 2m50s | 6m | 11m32s |
| | 15 | 15/15 | 2 | 7.2 | 9.2 | 0.0 | 3m | 11m | 18m2s |
| | 25 | 15/15 | 2 | 7.6 | 9.6 | 0.0 | 2m50s | 13m38s | 24m8s |
| 5-4/16/15- | 5 | 12/12 | 2.2 | 7.4 | 9.7 | 0.0 | 2m16s | 7m | 11m39s |
| | 10 | 12/12 | 2.2 | 7.1 | 9.3 | 0.0 | 2m34s | 6m41s | 11m29s |
| | 15 | 12/12 | 2.3 | 7.2 | 9.5 | 0.01 | 2m28s | 10m7s | 17m29s |
| | 25 | 12/12 | 2 | 7 | 9 | 0.01 | 8m30s | 22m39s | 38m21s |
| 5-4/8/20- | 5 | 24/24 | 2.1 | 8.9 | 11 | 0.0 | 2m | 33m | 36m |
| | 10 | 24/24 | 2 | 8.7 | 10.7 | 0.0 | 2m30s | 55m54s | 1h2m |
| | 15 | 24/24 | 2 | 8.8 | 10.8 | 0.0 | 2m27s | 1h38m | 1h46m |
| | 25 | 24/24 | 2.1 | 9 | 11.1 | 0.0 | 4m20s | 1h45m | 2h |
| 5-4/12/20- | 5 | 15/15 | 2 | 9.4 | 11.4 | 0.01 | 1m50s | 35m32s | 39m9s |
| | 10 | 15/15 | 2.2 | 8.6 | 10.8 | 0.0 | 2m56s | 1h19m | 1h25m |
| | 15 | 15/15 | 2.6 | 8.6 | 11.2 | 0.01 | 7m7s | 1h57m | 2h11m |
| | 25 | 15/15 | 2 | 8.2 | 10.2 | 0.0 | 4m27s | 1h19m | 1h34m |
| 5-4/16/20- | 5 | 12/12 | 2 | 8.9 | 10.9 | 0.0 | 4m38s | 22m32s | 29m2s |
| | 10 | 12/12 | 2.1 | 9.8 | 11.9 | 0.0 | 4m2s | 1h2m | 1h10m |
| | 15 | 12/12 | 2.5 | 9.8 | 12.3 | 0.0 | 16m30s | 2h26m | 2h49m |
| | 25 | 12/12 | 2.4 | 9.9 | 12.3 | 0.01 | 1h16m | 3h58m | 5h25m |

Table 11: Detailed results for 5-4/12/15-25-, 5-4/12/20-25- and 5-4/12/50-15-

| | | 5-4/12/15-25- | | | | 5-4/12/20-25- | | | | 5-4/12/50-15- | | | |
|---|---|---|---|---|---|---|---|---|---|---|---|---|---|
| | | ub | lb | Gap(%) | Time | ub | lb | Gap(%) | Time | ub | lb | Gap(%) | Time |
| (I2, LT, TC, NIT) | 1 | 71146.4 | 71146.4 | 0.00 | 8m52s | 76597.5 | 76597.5 | 0.00 | 1h50m | 192216.0 | 192136.0 | 0.04 | 11h9m |
| | 2 | 75246.1 | 75246.1 | 0.00 | 9m36s | 90515.9 | 90489.4 | 0.03 | 13m5s | 183250.0 | 183165.0 | 0.05 | 57h16m |
| | 3 | 82505.5 | 82505.5 | 0.00 | 10m12s | 84316.8 | 84316.8 | 0.00 | 1h2m | 190410.9 | 190228.3 | 0.10 | - |
| **average** | | 76299.3 | 76299.3 | 0.00 | 9m33s | 83810.1 | 83801.2 | 0.01 | 1h2m | 188625.6 | 188509.8 | 0.06 | 34h12m |
| (I1, LT, TC, NIT) | 1 | 69862.2 | 69862.2 | 0.00 | 9m51s | 79842.3 | 79842.3 | 0.00 | 17m30s | 188827.0 | 188539.1 | 0.15 | - |
| | 2 | 75536.5 | 75536.5 | 0.00 | 9m39s | 88416.3 | 88416.3 | 0.00 | 15m41s | 182033.0 | 181944.0 | 0.05 | 5h36m |
| | 3 | 76998.7 | 76998.7 | 0.00 | 9m48s | 82822.0 | 82822.0 | 0.00 | 15m33s | 188881.3 | 188686.4 | 0.10 | - |
| **average** | | 74132.5 | 74132.5 | 0.00 | 9m46s | 83693.5 | 83693.5 | 0.00 | 16m14s | 186580.4 | 186389.8 | 0.10 | 5h36m |
| (I1, HT, TC, NIT) | 1 | 98256.0 | 98256.0 | 0.00 | 9m35s | 117079.0 | 117079.0 | 0.00 | 19m21s | 275113.3 | 272759.1 | 0.86 | - |
| | 2 | 105654.0 | 105654.0 | 0.00 | 10m28s | 126107.0 | 126098.0 | 0.01 | 14m36s | 263067.0 | 262956.0 | 0.04 | 17h43m |
| | 3 | 109252.0 | 109251.0 | 0.00 | 10m28s | 119896.0 | 119896.0 | 0.00 | 23m55s | 272392.7 | 269664.1 | 1.00 | - |
| **average** | | 104387.3 | 104387.0 | 0.00 | 10m44s | 121027.3 | 121024.3 | 0.00 | 19m17s | 270191.0 | 268459.7 | 0.63 | 17h43m |
| (I1, LT, LC, NIT) | 1 | 85410.0 | 85410.0 | 0.00 | 10m1s | 92902.8 | 92902.8 | 0.00 | 13m31s | 190269.0 | 190259.0 | 0.01 | 36m44s |
| | 2 | 85285.8 | 85285.8 | 0.00 | 9m19s | 93485.5 | 93485.5 | 0.00 | 13m23s | 180619.0 | 180619.0 | 0.00 | 34m56s |
| | 3 | 83886.4 | 83886.4 | 0.00 | 9m42s | 89401.7 | 89401.7 | 0.00 | 13m15s | 190580.0 | 190551.0 | 0.02 | 36m55s |
| **average** | | 84860.7 | 84860.7 | 0.00 | 9m40s | 91930.0 | 91930.0 | 0.00 | 13m23s | 187156.0 | 187143.0 | 0.01 | 36m12s |
| (I1, LT, TC, NVT) | 1 | 71174.0 | 71174.0 | 0.00 | 9m31s | 96847.2 | 96847.2 | 0.00 | 13m32s | 181685.2 | 181146.7 | 0.30 | - |
| | 2 | 56085.6 | 56085.6 | 0.00 | 9m4s | 92481.1 | 92481.1 | 0.00 | 20m45s | 214547.0 | 214475.0 | 0.03 | 36h21m |
| | 3 | 77253.9 | 77253.9 | 0.00 | 9m47s | 92953.2 | 92953.2 | 0.00 | 23m41s | 194353.6 | 194160.2 | 0.10 | - |
| **average** | | 68171.2 | 68171.2 | 0.00 | 9m27s | 94093.8 | 94093.8 | 0.00 | 19m19s | 196861.9 | 196594.0 | 0.14 | 36h21m |

Table 12: Detailed results for 5-4/16/15-25-, 5-4/16/20-25- and 5-4/16/50-15-

| | | 5-4/16/15-25- | | | | 5-4/16/20-25- | | | | 5-4/16/50-15- | | | |
|---|---|---|---|---|---|---|---|---|---|---|---|---|---|
| | | ub | lb | Gap(%) | Time | ub | lb | Gap(%) | Time | ub | lb | Gap(%) | Time |
| (I1, LT, TC, NIT) | 1 | 68308.6 | 68308.6 | 0.00 | 10m31s | 77457.4 | 77457.4 | 0.00 | 14m40s | 176344.0 | 176273.0 | 0.04 | 4h10m |
| | 2 | 68268.8 | 68268.8 | 0.00 | 9m31s | 83721.4 | 83721.4 | 0.00 | 45m22s | 174587.0 | 174570.0 | 0.01 | 6h30m |
| | 3 | 69865.8 | 69865.8 | 0.00 | 9m43s | 84059.2 | 84059.2 | 0.00 | 31m36s | 182674.0 | 182632.0 | 0.02 | 19h38m |
| **average** | | 68814.4 | 68814.4 | 0.00 | 9m55s | 81746.0 | 81746.0 | 0.00 | 30m32s | 177868.3 | 177825.0 | 0.02 | 10h6m |
| (I1, HT, TC, NIT) | 1 | 97063.5 | 97063.5 | 0.00 | 10m47s | 115242.0 | 115242.0 | 0.00 | 14m35s | 261513.0 | 261384.0 | 0.05 | 6h28m |
| | 2 | 97640.0 | 97640.0 | 0.00 | 11m3s | 122079.0 | 122025.0 | 0.04 | 1h55m | 254798.0 | 254725.0 | 0.03 | 29h1m |
| | 3 | 102520.0 | 102491.0 | 0.03 | 9m57s | 120723.0 | 120723.0 | 0.00 | 48m17s | 267690.8 | 265847.9 | 0.69 | - |
| **average** | | 99074.5 | 99064.8 | 0.01 | 10m35s | 119348.0 | 119330.0 | 0.01 | 59m22s | 261333.9 | 260652.3 | 0.26 | 17h44m |
| (I1, LT, LC, NIT) | 1 | 84768.3 | 84768.3 | 0.00 | 9m16s | 92933.6 | 92933.6 | 0.00 | 14m26s | 187444.0 | 187444.0 | 0.00 | 43m30s |
| | 2 | 68358.8 | 68358.8 | 0.00 | 9m18s | 79351.7 | 79351.7 | 0.00 | 15m57s | 151987.0 | 151987.0 | 0.00 | 39m28s |
| | 3 | 69606.2 | 69606.2 | 0.00 | 10m12s | 75279.5 | 75279.5 | 0.00 | 22m14s | 158576.0 | 158522.0 | 0.03 | 52m5s |
| **average** | | 74244.4 | 74244.4 | 0.00 | 9m35s | 82521.6 | 82521.6 | 0.00 | 17m32s | 166002.3 | 165984.3 | 0.01 | 45m1s |
| (I1, LT, TC, NVT) | 1 | 69772.4 | 69748.9 | 0.03 | 9m10s | 93171.1 | 93171.1 | 0.00 | 13m58s | 169987.0 | 169949.0 | 0.02 | 11h46m |
| | 2 | 52241.9 | 52241.9 | 0.00 | 9m18s | 86603.9 | 86560.8 | 0.01 | 18m1s | 206768.8 | 206072.7 | 0.34 | - |
| | 3 | 69025.6 | 69025.6 | 0.00 | 9m14s | 85880.8 | 85880.8 | 0.00 | 16m55s | 192274.7 | 191670.8 | 0.31 | - |
| **average** | | 63680.0 | 63672.1 | 0.01 | 9m14s | 90003.9 | 90003.9 | 0.00 | 16m18s | 189676.8 | 189230.8 | 0.22 | 11h46m |

Table 13: Location decisions and their operating periods for 5-4/./15-25-(.,.,.,.)-3

| | (I1,LT,TC,NIT) | | | (I1,HT,TC,NIT) | | | (I1,LT,TC,NVT) | | | (I1,LT,LC,NIT) | | | Presence (%) |
|---|---|---|---|---|---|---|---|---|---|---|---|---|---|
| $\|\mathcal{L}\|$ | 8 | 12 | 16 | 8 | 12 | 16 | 8 | 12 | 16 | 8 | 12 | 16 | |
| l1 | 0 | 0 | 0 | 0 | 0 | 0 | 0 | 0 | 0 | 0 | 0 | 0 | 0 |
| l2 | 0 | 0 | 0 | 0 | 0 | 0 | 0 | 0 | 0 | 0 | 0 | 0 | 7 |
| l3 | 0 | 0 | 0 | 0 | 0 | 0 | 0 | 0 | 0 | 0 | 0 | 0 | 0 |
| l4 | 1 | 0 | 1 | 1 | 0 | 1 | 1 | 0 | 1 | 0 | 0 | 0 | 50 |
| l5 | 0 | 0 | 0 | 0 | 0 | 0 | 0 | 0 | 0 | 1 | 0 | 0 | 7 |
| l6 | 3 | 0 | 0 | 3 | 0 | 0 | 1 | 0 | 0 | 0 | 0 | 0 | 36 |
| l7 | 0 | 4 | 0 | 0 | 4 | 0 | 0 | 2 | 0 | 0 | 1 | 0 | 36 |
| l8 | 0 | 0 | 0 | 0 | 0 | 0 | 0 | 0 | 0 | 0 | 0 | 0 | 0 |
| l9 | | 0 | 0 | | 0 | 0 | | 0 | 0 | | 0 | 0 | 0 |
| l10 | | 0 | 0 | | 0 | 0 | | 0 | 0 | | 0 | 0 | 0 |
| l11 | | 0 | 0 | | 0 | 0 | | 0 | 0 | | 0 | 0 | 0 |
| l12 | | 1 | 0 | | 1 | 0 | | 1 | 0 | | 0 | 0 | 14 |
| l13 | | | 0 | | | 0 | | | 0 | | | 0 | 0 |
| l14 | | | 0 | | | 0 | | | 0 | | | 1 | 7 |
| l15 | | | 0 | | | 0 | | | 0 | | | 0 | 0 |
| l16 | | | 3 | | | 3 | | | $2^\star$ | | | 0 | 21 |
| Closet at t= | | | | | | | | | 4 | | | | |

Table 14: Location decisions under static modeling approach for 5-4/./20-25-(.,.,.,.)-3

| | (I1,LL,TC,NIT) | | (I1,HL,TC,NIT) | | (I1,LL,TC,NVT) | |
|---|---|---|---|---|---|---|
| $\|\mathcal{L}\|$ | 8 | 12 | 8 | 12 | 8 | 12 |
| l1 | 0 | 0 | 0 | 0 | 0 | 0 |
| l2 | 0 | 0 | 0 | 0 | 1 | 0 |
| l3 | 0 | 0 | 0 | 0 | 1 | 1 |
| l4 | 1 | 0 | 1 | 0 | 0 | 0 |
| l5 | 0 | 0 | 0 | 0 | 0 | 0 |
| l6 | 1 | 0 | 1 | 0 | 0 | 0 |
| l7 | 0 | 1 | 0 | 1 | 0 | 1 |
| l8 | 0 | 0 | 0 | 0 | 0 | 0 |
| l9 | | 0 | | 0 | | 0 |
| l10 | | 0 | | 0 | | 0 |
| l11 | | 0 | | 0 | | 0 |
| l12 | | 1 | | 1 | | 0 |